Article

Not peer-reviewed version

Enhanced Antioxidant and Anti-Glycation Abilities of Beeswax Alcohol in Reconstituted High-Density Lipoprotein with Potent Wound-Healing Activity and Protection of Embryo from Acute Toxicity of Carboxymethyllysine in Zebrafish

Kyung-Hyun Cho *, Seung-Hee Baek, Hyo-Seon Nam, Ashutosh Bahuguna

Posted Date: 28 September 2023

doi: 10.20944/preprints202309.2010.v1

Keywords: Beeswax alcohol (BWA); High-density lipoproteins (HDL); Reconstituted HDL; Carboxymethyllysine (CML); Zebrafish; Embryo

Article

Enhanced Antioxidant and Anti-Glycation Abilities of Beeswax Alcohol in Reconstituted High-Density Lipoprotein with Potent Wound-Healing Activity and Protection of Embryo from Acute Toxicity of Carboxymethyllysine in Zebrafish

Kyung-Hyun Cho [1,*], Seung-Hee Baek [1], Hyo-Seon Nam [1] and Ashutosh Bahuguna [1]

Raydel Research Institute, Medical Innovation Complex, Daegu 41061, Republic of Korea

* Correspondence: chok@raydel.co.kr. Tel: +82-53-964-1990, Fax: +82-53-965-1992

Abstract: The antioxidant and anti-inflammatory abilities of beeswax alcohol (BWA) are well reported in animal and human clinical studies, with a significant decrease in malondialdehyde (MDA) in blood, reduction of liver steatosis, and decrease in insulin. On the other hand, there is insufficient information to explain the in vitro antioxidant activity of BWA because it is extremely insoluble in aqueous buffer system. The BWA mixture was incorporated into reconstituted HDL (rHDL) with apoA-I, and the physiological functions of BWA in a water system were evaluated. After synthesis of rHDL with palmitoyloleoyl phosphatidylcholine (POPC), cholesterol, apolipoprotein A-I (apoA-I), and the BWA at molar ratios of 95:5:1:0 (rHDL-0), 95:5:1:0.5 (rHDL-0.5), and 95:5:1:1 (rHDL-1) for POPC:FC:apoA-I:BWA, the particle size of rHDL-1 was increased 15% compared to rHDL-0. rHDL-1 exhibited the strongest anti-glycation activity, up to 18% less glycation than rHDL-0 treated HDL_3, with the highest protection of apoA-I from proteolytic degradation: a 28% larger band intensity than that of rHDL-0 treated HDL_3 in the presence of fructose (final 250 mM). The antioxidant ability to inhibit cupric ion-mediated LDL oxidation increased as the BWA content in rHDL increased. The rHDL-1-treated LDL exhibited the smallest oxidation extent in electromobility with the least quantification of oxidized species (MDA). The antioxidant activities of HDL, ferric ion reduction ability (FRA), and paraoxonase (PON) were enhanced by the BWA in rHDL treatment with a concomitant increase in the molar ratio. rHDL-1-treated HDL showed 20–22% higher FRA and PON activities than rHDL-0-treated HDL. A microinjection of each rHDL into zebrafish embryos was performed in the presence of carboxymethyllysine (CML). The rHDL-1 injected embryo exhibited the highest survivability (~63%), whereas the CML alone group showed 28% survivability. A higher BWA content in rHDL helped neutralize the CML toxicity, resulting in higher survivability and normal developmental morphology. In contrast, the CML alone injected embryo showed severe retardation of the developmental speed and morphological defect. The CML-alone group showed the highest extent of reactive oxygen species (ROS) production and cellular apoptosis in embryos, but a co-injection of rHDL-1 resulted in a remarkable decrease in ROS and apoptosis. The dermal application of rHDL containing BWA resulted in higher potent wound-healing activity in a dose-dependent manner with decreased reactive oxygen species and cellular apoptosis in the cutaneous wound area in the presence of CML. Conclusively, incorporating BWA in rHDL significantly enhanced the anti-glycation and antioxidant activities in rHDL via more stabilization of apoA-I with a larger particle size. The rHDL containing BWA facilitated enforced inherent antioxidant ability of HDL and anti-inflammatory activity to suppress the CML toxicities in zebrafish embryos and to ameliorate CML-aggravated chronic wounds in adult zebrafish.

Keywords: Beeswax alcohol (BWA); High-density lipoproteins (HDL); Reconstituted HDL; Carboxymethyllysine (CML); Zebrafish; Embryo

1. Introduction

Many hydrophilic antioxidants, such as vitamin C, allicin, and melatonin, have been developed and marketed to react with oxidants in the cell cytoplasm and the blood plasma [1]. On the other hand, water-soluble antioxidants have limitations in inhibiting lipid peroxidation in the cell

 doi:10.20944/preprints202309.2010.v1

membranes because of the low interaction with the hydrophobic interface [2]. The development of lipid-soluble antioxidants is more advantageous to prevent oxidative damage to the cell membrane in a nonpolar environment [3]. Many chronic aging-related diseases are frequently associated with oxidative damage in cell membranes by reactive oxygen and nitrogen species [4,5], which have amphipathic properties between water and lipid interfaces. On the other hand, lipid-soluble antioxidants, such as carotenoids, vitamin E, coenzyme Q_{10} (CoQ_{10}), docosahexaenoic (DHA), and beeswax alcohol (BWA), are well-known nutrients with the potential to protect the cell membrane and to treat chronic aging-related diseases, such as cardiovascular disease (CVD), diabetes, and neurodegenerative diseases [6]. These compounds may prevent the cell membranes from damage by free radicals by readily scavenging peroxyl radicals, preventing lipid and protein oxidation in the amphipathic interface of plasma membrane in brain cells, neurons, and glia [7]. Nevertheless, in vitro evidence has not been sufficiently accumulated to prove the mechanistic insight of the antioxidants due to their low solubility in water.

Beeswax alcohol (BWA), a substance purified from beeswax, contains a mixture of six primary aliphatic alcohols (C24, C26, C28, C30, C32, and C34) with antioxidant, anti-platelet, cholesterol-lowering, and gastroprotective effects [8,9]. In particular, BWA supplementation promoted the secretion and quality of gastric mucus in ethanol-ulcer rat models and attenuated inflammation in antigen-induced arthritis [10,11]. With these properties, BWA has been registered as a functional food ingredient to help protect the body from oxidative stress, maintain a healthy stomach by protecting the gastric mucosa, and maintain joint health in Korean health functional foods according to the Ministry of Food and Drug Safety (MFDS, https://www.foodsafetykorea.go.kr/portal/board/boardDetail.do?menu_grp=MENU_NEW01&menu_no=2660&bbs_no=bbs987&nticmatr_yn=N&bbs_type_cd=01&ans_yn=N&ntctxt_no=21590). Oral acute treatment with BWA (5–100 mg/kg) reduces gastric ulceration and malondialdehyde (MDA) formation, a marker of lipid peroxidation, in the gastric mucosa of rats with indomethacin or ischemia reperfusion-induced ulcers [12,13]. The administration of BWA, 25–200 mg/kg, into rats by oral gavage revealed potent anti-inflammatory activity with a significant reduction of leukotriene B_4 (LTB_4) against carrageenan-induced pleuritic inflammation [14].

An in vitro assay of the BWA has been a limitation in evaluating the antioxidant capacity because of their extreme insolubility in the physiological aqueous buffer system. An isotonic aqueous buffer was selected to solubilize BWA for enzyme assay, cell-based assay, and animal experiments. The hurdle was overcome by incorporating BWA into reconstituted high-density lipoproteins (rHDL) with apoA-I to evaluate the antioxidant capacities of BWA in the physiological buffer system, according to a previous report [15]. The current study compared the in vitro effects of rHDL containing BWA (BWA-rHDL) and encapsulation of BWA into rHDL particles on the anti-glycation, antioxidant, and anti-inflammatory activities. The anti-glycation activity of BWA-rHDL was evaluated by testing the fructose or carboxymethyllysine (CML)-mediated glycation with HDL, which causes inflammation with neurotoxicity [16]. Among the AGE, an elevated serum *N*-ε-carboxymethyllysine (CML) level was also associated with the exacerbation of atherosclerosis via lipoprotein modifications and increased susceptibility of low-density lipoproteins (LDL) oxidation [17]. The antioxidant properties of the BWA have been compared using zebrafish embryos by testing the developmental speed, swimming ability, and survivability after the injection of the rHDL-BWA in the presence of the CML. Zebrafish embryos have well-developed innate and acquired immune systems like mammalian ones [18]. An additional advantage of working with zebrafish embryos is external development and optically transparent during development. With these characteristics, zebrafish and their embryos are a valuable and popular animal model for various studies, including screening of antioxidants [19], wound healing [20], and tissue regeneration [21].

This study was designed to compare the physicochemical characterizations of BWA-rHDL regarding particle size, morphology, and electromobility with the increased molar ratio of BWA. Each rHDL was evaluated in terms of the structural and functional correlations, antioxidant, anti-glycation, and anti-inflammatory activity in vitro and in vivo using zebrafish embryos and adults

 doi:10.20944/preprints202309.2010.v1

under acute hyperinflammation to provide information on the antioxidant and anti-inflammatory of BWA in HDL in the physiological potential.

2. Materials and Methods

2.1. Materials

Palmitoyloleoylphosphatidylcholine (POPC, #850457) was provided by Avanti Polar Lipids (Alabaster, AL, USA). Sodium cholate (#1254) and fructose (Cat #F0127) were purchased from Sigma-Aldrich (St. Louis, MO, USA). Purified beeswax alcohol (BWA, purity >90%) was obtained from the National Center for Scientific Research (CNIC), Havana, Cuba, via Raydel Pty, Ltd. (Thornleigh, NSW, Australia). The BWA material contained six high-molecular-weight alcohols purified from beeswax (from *Apis mellifera, L.*) with the following composition: tetracosanol (6–15%), hexacosanol (7–20%), octacosanol (12–20%), triacontanol (25–35%), dotriacontanol (18–25%), and tetratriacontanol (≤7.5%) (purity ≥ 85%) [22].

2.2. Purification of human lipoproteins

The different serum lipoproteins fractions, i.e., LDL ($1.019 < d < 1.063$) and HDL ($1.063 < d < 1.225$), were isolated from the blood samples of healthy individuals (average age 23±2 year). The blood was donated voluntarily by the participants after 12 hours of fasting and collected according to Helsinki guidelines approved by the Institutional Review Board of Korea National Institute for Bioethics Policy (KoNIBP, approval number P01-202109-31-009) supported by the Ministry of Health Care and Welfare (MOHW) of Korea. Different lipoprotein fractions from the blood were segregated by density gradient ultracentrifugation, where different density zones were prepared using NaCl and NaBr according to the standard method [23]. Briefly, serum (plasma) was ultracentrifuged at 100,000×g for 24 hr at 10°C. The separated lipoproteins were individually collected and processed for dialysis to remove the traces of NaBr against Tris-buffered saline (pH 8.0).

2.3. Purification of human apoA-I

ApoA-I was purified from HDL using the method reported by Brewer et al. [24], which involved organic solvent extraction, ultracentrifugation, and column chromatography. The protein purity was confirmed to be at least 95% according to SDS-PAGE analysis.

2.4. Synthesis of reconstituted HDL

Reconstituted HDL (rHDL) was prepared using the sodium cholate dialysis method [25], with initial molar ratios of 95:5:1:0, 95:5:1:0.5, and 95:5:1:1 for POPC:cholesterol:apoA-I:BWA, respectively.

2.5. Protein determination

The protein content of purified HDL and LDL was obtained through ultracentrifugation, and the reconstituted HDL was analyzed using the Lowry assay according to a slight modification of the method reported by Markwell et al. [26]. Bovine serum albumin (BSA) was used as a standard for calibration. Lipid-free apoA-I was quantified using the Quick Start™ Bradford Protein Assay Kit (Bio-Rad #5000201), with BSA as the standard.

2.6. Oxidation of LDL

Oxidized LDL (oxLDL) was generated by incubating the human LDL (1 mg/mL) with $CuSO_4$ (Sigma #451657) at a final concentration of 10 μM for four hours at 37 °C. After incubation, the oxLDL was filtered using a 0.22-μm filter and analyzed to measure the extent of oxidation using a thiobarbituric acid reactive substances (TBARS) assay [27] with malondialdehyde (MDA, Sigma #63287) standard.

The antioxidant capacity of each rHDL was tested in the presence of Cu^{2+} (final 10 μM) by comparing their electromobility on a 0.5% agarose gel [28]. The relative electromobility was

 doi:10.20944/preprints202309.2010.v1

compared by mixing 25 μg of LDL protein and 5 μg of each rHDL protein, followed by electrophoresis under non-denatured conditions. Electrophoresis was performed at 50 V for 1 hr in Tris-acetate-EDTA buffer (pH 8.0). Apo-B in LDL was visualized by Coomassie brilliant blue staining (final concentration 1.25%). Oxidized LDL migrated faster towards the bottom of the gel due to apo-B fragmentation and increased the negative charge.

2.7. Characterization of Trp fluorescence in the rHDL

The wavelengths of maximum fluorescence (WMF) of the tryptophan (Trp) residues in apoA-I, both in its lipid-free and lipid-bound states, were determined using an FL6500 spectrofluorometer (Perkin-Elmer, Norwalk, CT, USA). The samples were excited at 295 nm to avoid interference from tyrosine fluorescence, and the emission spectra were recorded from 305 to 400 nm at room temperature, according to a previous report [15,16].

2.8. Glycation of HDL in the presence of the rHDL containing BWA

The anti-glycation activity of lipid-free BWA was tested by conducting glycation by incubating the purified HDL$_2$ (final 2 mg/mL of protein) with CML (final 400 μM) at 37°C in an atmosphere containing 5% CO_2 for up to 144 hr in 200 mM potassium phosphate/0.02% sodium azide buffer (pH 7.4). The anti-glycation activity was tested by incubating lipid-free BWA (final 10, 20, and 30 μM) in the same buffer with the HDL and CML. The apoA-I content was compared using SDS-PAGE (5 μg of apoA-I in a lipid-bound state or 7 μg of apoA-I in a lipid-free state per lane) and densitometric analysis because glycation resulted in a severe decrease in the protein content in HDL and several beneficial functions of apoA-I [16]. The extent of the advanced glycation reactions was determined by reading the fluorescence intensities at 370 nm (excitation) and 440 nm (emission), as described previously [29]. The BI was compared by band scanning with Chemi-Doc® XR (Bio-Rad) using Quantity One software (version 4.5.2) from three independent SDS-PAGE analyses.

Purified HDL (final concentration 2 mg/mL) was incubated with 250 mM D-fructose (Sigma #F2793) in a 200 mM potassium phosphate/0.02% sodium azide buffer (pH 7.4) using a previously published method reported elsewhere to compare the anti-glycation sensitivity of BWA in rHDL state [29]. The glycated mixture sample was incubated for up to 96 hours in an atmosphere containing 5% CO_2 at 37 °C. The extent of the advanced glycation reactions was determined by measuring the fluorescence intensities at 370 nm (excitation) and 440 nm (emission) using an FL6500 spectrofluorometer (Perkin-Elmer, Norwalk, CT, USA) with Spectrum FL software version 1.2.0.583 (Perkin-Elmer) and a 1 cm path-length Suprasil quartz cuvette (Fisher Scientific, Pittsburgh, PA, USA).

2.9. Zebrafish maintenance

Zebrafish and their embryos were maintained using standard protocols [30] and in compliance with the Guide for the Care and Use of Laboratory Animals [31]. All zebrafish-related procedures and maintenance were approved by the Committee of Animal Care and Use of Raydel Research Institute (approval code RRI-20-003, Daegu, Republic of Korea). The zebrafish were housed in a temperature-controlled system tank at 28 °C and subjected to a 10:14 hour light cycle. The fish were fed a regular diet of tetrabit granules (TetrabitGmbh D49304, containing 47.5% crude protein, 6.5% crude fat, 2.0% crude fiber, and 10.5% crude ash) supplemented with vitamin A (29,770 IU/kg), vitamin D3 (1860 IU/kg), vitamin E (200 mg/kg), and vitamin C (137 mg/kg) from Melle, Germany.

2.10. Microinjection of CML and rHDL into Zebrafish Embryos

One-day post-fertilization (dpf) zebrafish embryos were microinjected individually using a pneumatic picopump (PV830; World Precision Instruments, Sarasota, FL, USA) equipped with a magnetic manipulator (MM33; Kantec, Bensenville, IL, USA) and a pulled microcapillary pipette-using device (PC-10; Narishigen, Tokyo, Japan). An injection of each rHDL alone (16 μg of apoA-I) or co-injection with CML (800 ng) was performed at the same location in the yolk to minimize bias,

 doi:10.20944/preprints202309.2010.v1

following a previously described method [15,20]. After the injection, the live embryos were observed under a stereomicroscope (Zeiss Stemi 305, Oberkochen, Germany) and photographed at 20× magnification using a Motic cam2300 CCD camera. At 24 hours post-injection, the chorion was removed, and each live embryo was compared to assess the developmental stage at a higher magnification of 50×.

2.11. Imaging of Oxidative Stress, Apoptosis in Embryo

After injecting CML with each rHDL, the reactive oxygen species (ROS) levels and the extent of cellular apoptosis in the embryos were imaged by dihydroethidium (DHE) staining and acridine orange (AO) staining, respectively, as described elsewhere [32]. The images of the ROS were obtained by fluorescence observations (Ex = 585 nm and Em = 615 nm), as described previously [33]. The extent of cellular apoptosis among the groups was compared using acridine orange (AO) staining and fluorescence observations (Ex = 505 nm, Em = 535 nm), as reported elsewhere [34] using a Nikon Eclipse TE2000 microscope (Tokyo, Japan).

2.12. Cutaneous wound formation

A cutaneous wound was produced by anesthetizing 16-week-old zebrafish with 0.1% of 2-phenoxyethanol and removing the surface scale. A 2 mm-diameter cutaneous wound was produced using a biopsy punch (Kai industries co., Ltd., Oyana, Japan) at the left flank to the anal and dorsal fin region of the zebrafish. The wounded zebrafish were segregated randomly into five groups (n=15 in each group). The wound area of the zebrafish in Groups I and II was treated with 1 µL of PBS and 1 µL of 25 mg/mL CML (final 25 µg), respectively. The wound areas of the zebrafish in Groups III, IV, and V were treated with 1 µL of rHDL-0, rHDL-0.5, and rHDL-1 along with CML (final 25 µg), respectively. Three min post-treatment, the zebrafish were transferred into their respective tanks maintained at a 28°C water temperature.

2.13. Visual observation of wound healing

The wounded area of the zebrafish was persistently monitored at 0 hr, 2 hr, 4 hr,6 hr, 24 hr, and 48 hr after being stained with methylene blue as an earlier adopted method [20]. Briefly, at the respective time point, zebrafish were anesthetized by drenching into 0.1% of 2-phenoxyethanol and the subsequent addition of methylene blue (0.1% w/v, final 2 µL) at the wounded site. After one minute, the stained area was washed three times with water and visualized under a stereomicroscope (Motic SMZ 168; Hong Kong). The wound area (blue stained) was measured at different time points (2–48 hr). Wound healing was calculated by comparing the wound area (mm^2) at different time points with the wound area of 0 hr using Image J software (http://rsb.info.nih.gov/ij, version1.53r accessed on 16 July, 2023).

2.14. Statistical Analysis

The results are presented as the mean±SD from a minimum of three independent experiments with duplicate samples. Statistical analysis was performed using the SPSS software program (version 28.0; SPSS, Inc., Chicago, IL, USA). For the in vitro studies, the effects of each rHDL treatment were compared using an independent t-test. In the zebrafish study, the survival rates and fluorescence signals in the different groups were also compared using an independent t-test. A p-value < 0.05 was considered significant.

3. Results

3.1. Antioxidant ability of BWA against LDL oxidation

The cupric ion (final 10 ◎M) treatment of native LDL (lane N) caused the production of more oxidized LDL (lane O), resulting in faster electromobility to migrate to the bottom of the agarose gel due to increase of negative charge and apo-B fragmentation (Figure 1A). The co-treatment of vitamin

Preprints (www.preprints.org) | NOT PEER-REVIEWED | Posted: 28 September 2023 doi:10.20944/preprints202309.2010.v1

C (vit C) resulted adequate inhibition ability with slower electromobility and stronger band intensity (lane 3) than those of oxidized LDL. On the other hand, co-treatment of BWA (lanes 4–6) resulted in stronger antioxidant ability than vit C treatment to show the slowest electromobility and the strongest band intensity in a dose-dependent manner of BWA (lane 6). The quantification of malondialdehyde (MDA) in the LDL mixture showed that the BWA treatment caused a significant decrease in MDA in a dose-dependent manner up to 32% lower than oxidized LDL. In comparison, the vit C treatment showed only a 10% reduction at the final 30 ◎M treatment, as shown in Figure 1B. The treatment of BWA resulted in 25% lower MDA (p<0.001) than the vit-C treated LDL at the final 30 ◎M treatment in the presence of cupric ions and tween-20. These results showed that BWA had remarkably higher antioxidant ability than vit-C against the cupric ion-mediated LDL oxidation, suggesting the superior capability of BWA in a hydrophobic environment via lipophilic interaction with the LDL surface.

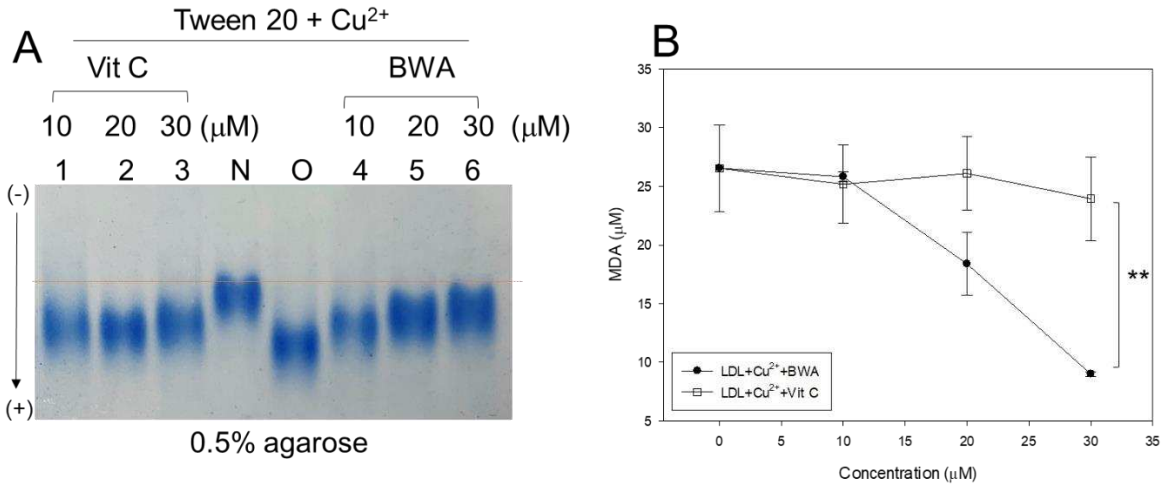

Figure 1. Comparison of the antioxidant ability between lipid-free BWA and vitamin C against cupric ion mediated LDL oxidation. A. Electromobility of LDL under a non-denatured state in the presence of Tween 20 and cupric ions with BWA or vit-C after 4 hr incubation at 37°C. Red-dotted line indicates the similar electromobility of native LDL (lane N) and BWA-treated ox-LDL (lane 6). B. Quantification of malondialdehyde in the LDL by thiobarbituric acid reactive substances (TBARS) assay. **, p<0.01.

3.2. Anti-glycation activity of BWA against CML-induced modification of HDL3

Lipid-free BWA exerted remarkable anti-glycation activity to suppress the production of yellowish fluorescence in a dose-dependent manner, with up to 11% and 13% inhibition of the fluorescence at 20 and 30 ◎M of BWA, respectively, at 144 hr incubation (Figure 2A). Interestingly, WMF of HDL was redshifted upon the CML treatment to 341 nm from 337 nm at the native state, suggesting that intrinsic Trp was exposed to the aqueous phase because of a disturbance of the tertiary structure by the glycation stress. On the other hand, the co-treatment of BWA caused a blue shift of WMF, especially around 338 nm at 30 ◎M of BWA, indicating the stabilization of apoA-I in the presence of BWA via the inhibition of glycation stress.

Electrophoresis of the HDL3 showed that the treatment of CML into HDL3 caused the remarkable degradation of the HDL3 band intensity with a slight up-shift the band position (lane 1) compared to native HDL3 (lane N), as shown in Figure 1B. On the other hand, the co-treatment of BWA caused notable protection of apoA-I from the CML-mediated proteolytic degradation in a dose-dependent manner: up to ~1.5-fold and 1.3-fold stronger band intensities at 72 hr and 144 hr, respectively. In addition, co-treatment of BWA resulted in more distinct band intensity of apoA-I and shifted down the band position similar to those of native apoA-I (lane N)

Preprints (www.preprints.org) | NOT PEER-REVIEWED | Posted: 28 September 2023 doi:10.20944/preprints202309.2010.v1

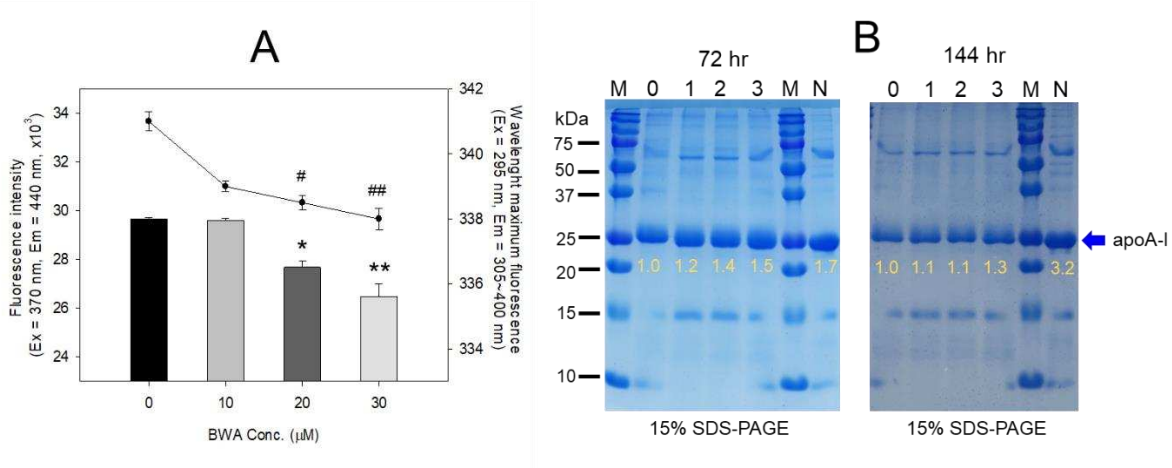

Figure 2. Anti-glycation ability of lipid-free BWA against CML-mediated glycation. A. Fluorescence intensity (Ex=370 nm, Em=440 nm) and wavelength maximum fluorescence (Ex=295 nm, Em=310-400 nm) of HDL_3 in the presence of CML (final 400 ⊙M) and BWA (final 10, 20, and 30 ⊙M) at 144 hr incubation. *, $p<0.05$ vs. HDL + CML; **, $p<0.05$ vs. HDL + CML; #, $p<0.05$ vs. HDL + CML; ##, $p<0.05$ vs. HDL + CML. B. Electrophoretic patterns of HDL in the presence of CML (final 400 ⊙M) and BWA (final 10, 20, and 30 ⊙M) at 72 hr and 144 hr incubation (15% SDS-PAGE). The protein bands were visualized by Coomassie blue staining. The red font indicates the band intensity of apoA-I from three independent SDS-PAGE. Lane N, native HDL; lane M, molecular weight marker (Bio-Rad, prestained low-range). .

3.3. Synthesis of reconstituted HDL containing BWA

BWA exhibited sufficient binding ability to phospholipid (PL) and apoA-I to form rHDL (Table 1), with a molar ratio of 95:5:1:0 (rHDL-0), 95:5:1:0.5 (rHDL-0.5), and 95:5:1:1 (rHDL-1) for POPC:FC:apoA-I:BWA; the particle size of rHDL-1 was increased significantly, 15% higher than rHDL-0. The rHDL-0 and rHDL-0.5 showed a similar particle size of approximately 61–65 nm of diameter with the same wavelength maximum fluorescence (WMF) 330.9–331.0 nm, indicating that the incorporation of low molar ratio of BWA did not significantly change the rHDL structure and intrinsic Trp108 movement of the amphipathic helix in apoA-I. Upon lipid-free apoA-I binding with cholesterol and phospholipid in the native state, the WMF of apoA-I was 5.4 nm blue-shifted from 336.3 nm to 330.9 nm of WMF, indicating that the intrinsic Trp108 in apoA-I was moved to a more nonpolar phase. On the other hand, incorporating BWA at a high molar ratio resulted in a slightly larger redshift of WMF around 331.4 nm, indicating that the Trp108 was more exposed and moved to the polar phase. After synthesis, each rHDL contained apoA-I (2 mg/mL) and rHDL-0.5, and rHDL-1 contained 12.5 μg/mL and 25 μg/mL of BWA, respectively.

Table 1. Characterization of rHDL containing different ratios of beeswax alcohol.

Name	MW of BWA[1] (Averaged)	Molar Ratio POPC:FC:apoA-I:BWA	WMF (nm)	Diameter (nm)
rHDL-0	-	95:5:1:0	330.9±0.1	61.2±1.6
rHDL-0.5	429.1	95:5:1:0.5	331.0±0.0	65.4±2.3
rHDL-1		95:5:1:1	331.4±0.1	70.5±2.3

BWA, beeswax alcohol; MW, molecular weight (averaged); POPC, palmitoyloleoyl phosphatidylcholine; FC, free cholesterol; WMF, wavelength maximum fluorescence. [1] Total amount of long-chain aliphatic alcohols in BWA: 859.79 mg/g, 1-tetracosanol (C24) : 63.67 mg/g, 1-hexacosanol (C26) : 114.28 mg/g, 1-octacosanol (C28) : 135.96 mg/g, 1-triacotanol (C30) : 292.25 mg/g, 1-dotriacotanol : 222.97 mg/g, residual aliphatic alcohol : 30.62 mg/g.

Preprints (www.preprints.org) | NOT PEER-REVIEWED | Posted: 28 September 2023 doi:10.20944/preprints202309.2010.v1

3.4. Electrophoretic profiles of rHDL containing BWA

As shown in Figure 3A, the synthesis of rHDL was well carried out: apoA-I band was up-shifted slightly upon binding with phospholipid and cholesterol (lane 2, 3, and 4) compared to lipid-free apoA-I (lane 1). The rHDL containing BWA showed a thicker band area and intensity in the bottom of the gel for debris of PL and BWA (PL+BWA) as the red arrow indicated: rHDL-0.5 and rHDL-1 showed 1.6- and 2.8-fold, respectively, higher band intensity than that of rHDL-0. The BWA exhibited sufficient binding ability with phospholipid and apoA-I with 17% and 53% more band intensity of apoA-I (lanes 3 and 4) than rHDL alone (lane 2), as shown in Figure 3A, indicating that more BWA binding is associated with, the more protection of apoA-I during the rHDL synthesis.

As shown in Figure 3B, under the native state, the three rHDL showed similar electromobility in 0.6% agarose, indicating that the three-dimensional structure of apoA-I and the electric charge distribution of rHDL particles were similar in all rHDL. On the other hand, rHDL-1 showed the strongest band intensity of apoA-I, while rHDL-0 showed the weakest band intensity. These results suggest that the greater incorporation of BWA in rHDL resulted in the stabilization of apoA-I and rHDL via the putative strong affinity binding of BWA and apoA-I with the darker band intensity, as shown in the blue arrow (Figure 3B).

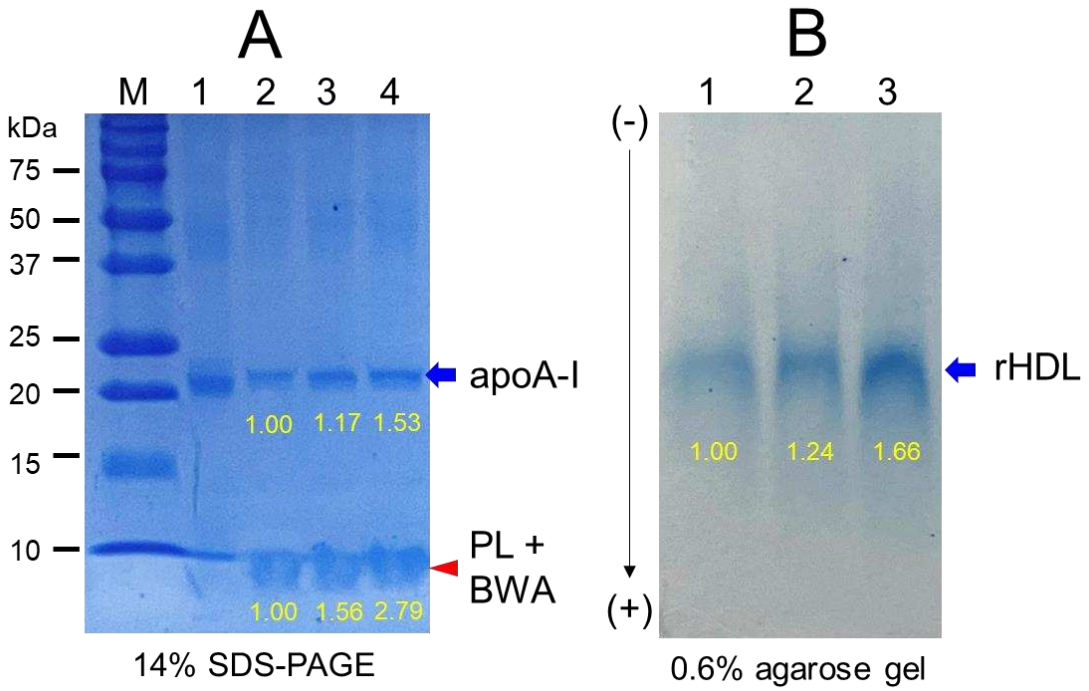

Figure 3. Electrophoretic profiles of rHDL containing BWA in the denatured state (A) and non-denatured state (B). A. Electrophoretic patterns of each rHDL under the denatured state on 14% SDS-PAGE (9 μg of protein/lane). The red arrowhead indicates phospholipid and BWA debris. The gel was stained by Coomassie brilliant blue (final 0.125%) staining to visualize apoA-I and phospholipid. Lane M, molecular weight standard (Precision plus protein standards, Bio-Rad Cat # 161-0374); lane 1, lipid-free apoA-I alone; lane 2, rHDL-0; lane 3, rHDL-0.5; lane 4, rHDL-1. B. Native electrophoresis of each rHDL under the non-denatured state on 0.6% agarose (10 μg of protein/lane) to compare the electromobility depends on the three-dimensional structure of apoA-I/HDL and its oxidation extent. The apoA-I in rHDL was visualized by Coomassie brilliant blue staining (final 1.25 %). Lane 1, rHDL-0; lane 2, rHDL- 0.5; lane 3, rHDL-1.

3.5. Electron microscopy observations

Transmission electron microscopy (TEM) showed that rHDL-0 (photo a) had a typical discoidal rHDL shape and rouleaux morphology with a scattered pattern (Figure 4). In contrast, rHDL-1 (photo c) showed the most distinct disc particle shape with long rouleaux morphology. In contrast, rHDL-

Preprints (www.preprints.org) | NOT PEER-REVIEWED | Posted: 28 September 2023 doi:10.20944/preprints202309.2010.v1

0.5 showed a smaller particle shape and short rouleaux morphology (photo c). The rHDL-0 and rHDL-0.5 showed similar particle sizes of 63–64 nm, but rHDL-1 showed the largest particle size with a homogeneous pattern around 70±2 nm in diameter (Inset graph D).

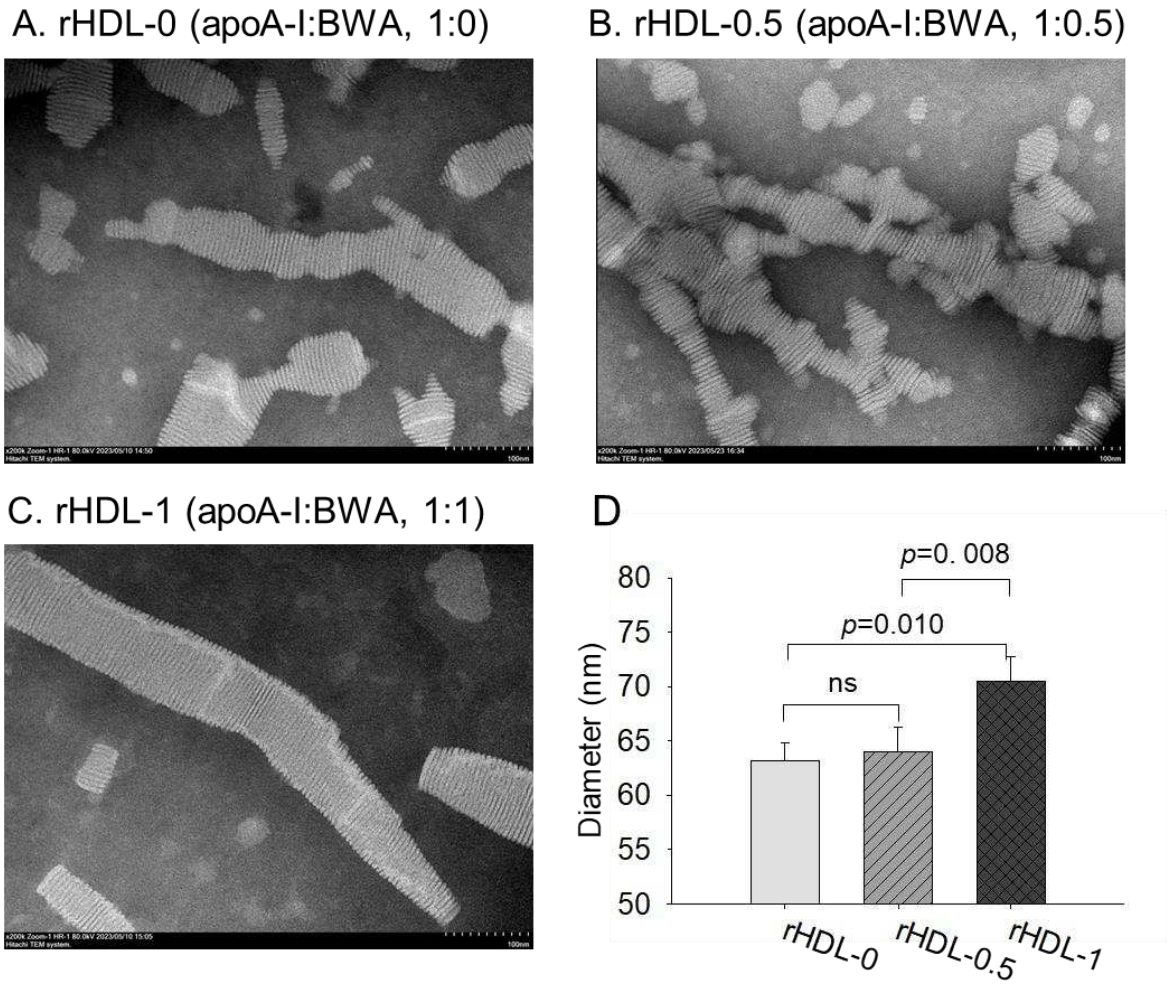

Figure 4. TEM image analysis of each rHDL containing BWA with 40,000× magnification. Among rHDLs, rHDL-1, (apoA-I: BWA, 1:1) (C) had the largest size, as shown in inset graph (D). The rHDL-1 exhibited the most distinct and uniform discoidal particle shape with a rouleaux pattern.

3.6. Anti-glycation activity of BWA in rHDL

Fructose (final 250 mM) treatment on human HDL caused severe glycation, with a seven-fold higher yellowish fluorescence intensity (FI) than HDL_2 alone during a 96 h incubation under 5% CO_2 (Figure 5A). On the other hand, the rHDL-1 treatment caused remarkable inhibition of the HDL_2 glycation, up to 26% lower (p<0.001) glycation extent than HDL alone at 96 h incubation, while other rHDLs showed 5–16% less inhibition than HDL_2 alone. Electrophoretic analysis with each HDL sample revealed the native HDL alone to have a distinct apoA-I band (28 kDa) at 0 hr (lane 1) and 72 hr (lane 2) without the fructose treatment (Figure 5B). Glycated HDL (lane 3) showed a remarkably diminished apoA-I band; 90% had disappeared after the fructose treatment. In contrast, the rHDL-0 co-treatment resulted in a 6% larger apoA-I band intensity than fructose-treated HDL_2, suggesting that rHDL alone had a low protection effect of apoA-I against the proteolytic degradation of glycation. On the other hand, rHDL containing BWA-treated HDL_2 showed a stronger band intensity of apoA-I with an increase in BWA content. Among rHDL, the rHDL-1 treated HDL (lane 6) showed the strongest band intensity: 28% more than rHDL-0. Hence, incorporating BWA in rHDL contributed to the protection of apoA-I from proteolytic degradation in a dose-dependent manner.

Preprints (www.preprints.org) | NOT PEER-REVIEWED | Posted: 28 September 2023 doi:10.20944/preprints202309.2010.v1

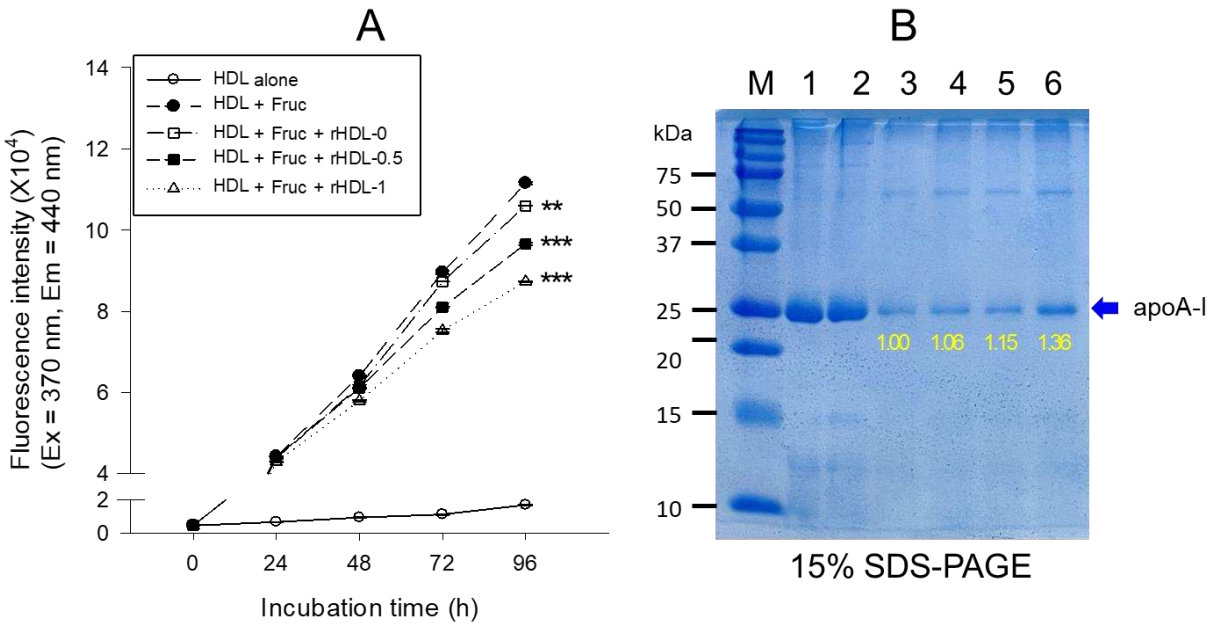

Figure 5. Anti-glycation activity of rHDL-containing BWA in fructose-treated HDL. A. Fluorescence spectroscopic analysis (Ex = 370 nm, Em = 440 nm) of HDL (1 mg/mL of protein), which was co-treated with fructose (final 250 mM) and each rHDL (0.2 mg/mL of apoA-I) containing BWA (final 1.3 and 2.6 μg/mL for rHDL-0.5 and rHDL-1, respectively) during 96 h incubation. The data were expressed as mean ± SD from three independent experiments with duplicate samples. ***, $p < 0.001$ vs. HDL_2 + Fruc. Each rHDL treatment was compared with HDL_2 + Fruc by independent *t*-test. B. Electrophoretic patterns of the HDL (5 μg/lane) after incubation with fructose and each rHDL (15% SDS-PAGE). M, molecular weight standard (Precision plus protein standards, Bio-Rad Cat # 161-0374). The protein bands were visualized by Coomassie brilliant blue (final 0.125%) staining. M represents molecular weight marker (kDa), lane 1, HDL alone (0 h); lane 2, HDL alone (72 h); lane 3, HDL + Fruc; lane 4, HDL + Fruc + rHDL-0; lane 5, HDL + Fruc + rHDL-0.5; and lane 6, HDL + Fruc + rHDL-1.

3.7. Antioxidant ability of BWA in rHDL against LDL oxidation

Native LDL showed the strongest band intensity with the slowest electromobility (lane N) (Figure 6A). In contrast, cupric ion (final 10 ◎M) treated LDL showed the weakest band intensity with the fastest electromobility (lane O). On the other hand, co-treatment of rHDL (lane 1) resulted in the slight attenuation of electromobility with a larger increase in the LDL band intensity, suggesting that rHDL alone had low antioxidant activity. The co-treatment of rHDL-0.5 (lane 2) and rHDL-1 (lane 3) resulted in slower electromobility with stronger band intensity than those of rHDL-0 (lane 1), suggesting that incorporation of BWA in the rHDL exerted more antioxidant activity to inhibit LDL oxidation. More oxidized LDL migrated faster towards the bottom of the gel from the loading position at the top, showing a more smeared and weaker band intensity of LDL caused by fragmentation of apo-B and an increase in negative charge in LDL.

Quantification of MDA in each LDL to determine the oxidation extent revealed the oxidized LDL (lane O) to have a 13-fold higher MDA level than native LDL (lane N), as shown in Figure 6B. On the other hand, the co-treatment of rHDL-0, rHDL-0.5, and rHDL-1 resulted in 9%, 24%, and 36% lower MDA than that of oxLDL, suggesting that incorporation of BWA in the rHDL exerted more antioxidant activity in a dose-dependent manner.

Preprints (www.preprints.org) | NOT PEER-REVIEWED | Posted: 28 September 2023 doi:10.20944/preprints202309.2010.v1

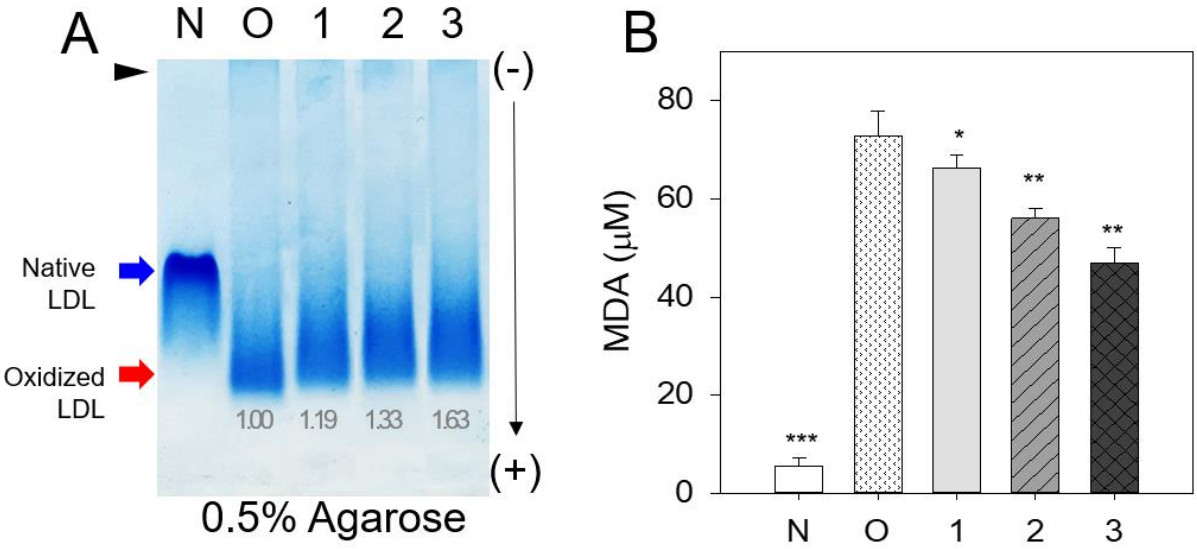

Figure 6. Comparison of the antioxidant abilities of rHDL-containing BWA during cupric-ion-mediated LDL oxidation. A. Comparison of the relative electromobility of a mixture of LDL (15 μg of protein) and each rHDL (6 μg of protein) under a non-natured state on 0.5% agarose gel (120 mm length × 60 mm width × 5 mm thickness). The electrophoresis was carried out with 50 V for 1 h in Tris-acetate-ethylene-diamine-tetra-acetic acid (EDTA) buffer (PH 8.0). The apo-B in LDL was visualized by Coomassie brilliant blue staining (final 1.25%). B. Extent of oxidation according to a TBARS assay with the malondialdehyde (MDA) standard. Each rHDL treatment was compared with LDL + $CuSO_4$ (oxLDL) by independent *t*-test. The data are expressed as mean ± SD from three independent experiments with duplicate samples. *, $p < 0.05$ vs. oxLDL alone **, $p < 0.01$ vs. oxLDL alone. lane N, native LDL; lane O, oxLDL; lane 1, LDL + $CuSO_4$ + rHDL-0; lane 2, LDL + $CuSO_4$ + rHDL-0.5; lane 3, LDL + $CuSO_4$ + rHDL-1.

3.8. Enhancement of antioxidant ability of HDL by rHDL containing BWA

The ferric ion reduction ability (FRA) of HDL (2 mg/mL) was enhanced by adding rHDL containing BWA, as shown in Figure 7A. HDL + rHDL-1 showed a 28% and 22% higher FRA than HDL alone and HDL + rHDL-0, respectively. HDL + rHDL-0.5 showed 12% and 7% higher FRA than that of HDL alone and HDL + rHDL-0, respectively, suggesting the synergistic effect of rHDL-containing BWA and HDL_3 depending on the BWA dose.

The HDL_3-associated paraoxonase (PON-1) assay showed that the addition of PBS or rHDL-0 (15 ◎g of apoA-I) resulted in similar PON activity of HDL_3 (20 ◎g of protein) of 93–95 ◎U/L/min (Figure 7B), suggesting that addition of the rHDL-0 did not elevate the PON activity. On the other hand, the addition of BWA in rHDL resulted in higher PON-1 activity: rHDL-0.5 and rHDL-1 showed 9% and 20% higher PON activity than that of rHDL-0 in HDL_3, respectively.

Preprints (www.preprints.org) | NOT PEER-REVIEWED | Posted: 28 September 2023 doi:10.20944/preprints202309.2010.v1

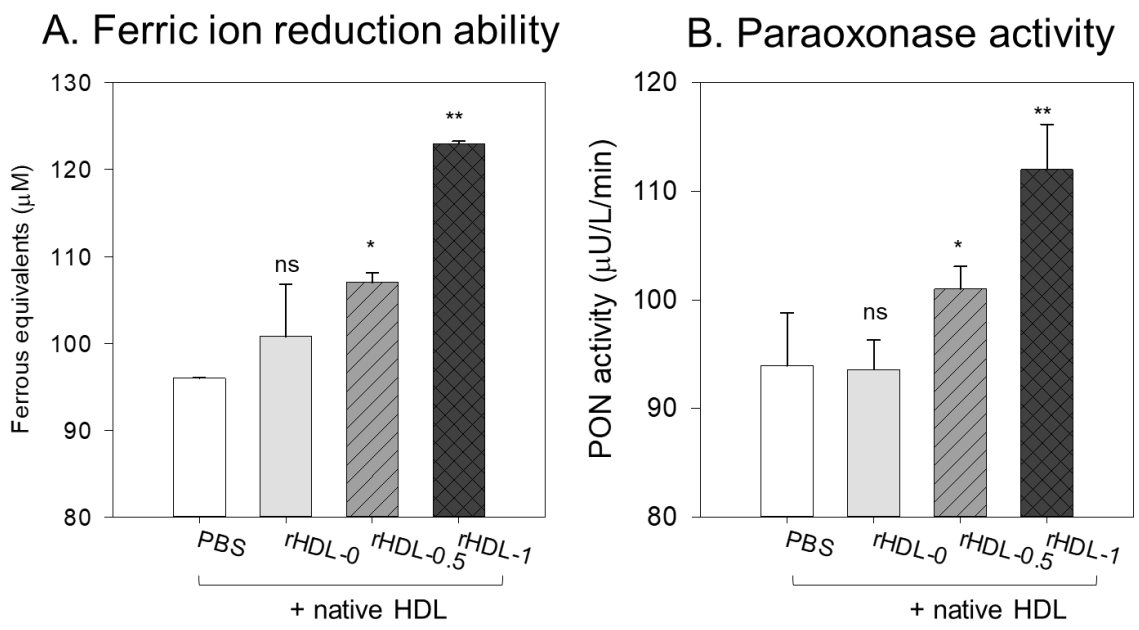

Figure 7. Comparison of the ferric ion reduction ability (FRA) (A) and the paraoxonase (PON-1) activity (B) in HDL. *, $p < 0.05$ vs. HDL alone; **, $p < 0.01$ vs. HDL alone; ns, not significant vs. HDL alone. A. The FRA activity was expressed as the equivalent concentration of vitamin C (μM), which is equivalent to reducing the amount of ferric ion (μM) per hour. B. The PON-1 activity was expressed as the initial velocity of *p*-nitrophenol production per min (μU/L/min) at 37 °C during 180 min of incubation. The data are expressed as the mean ± SD from three independent experiments with duplicate samples.

3.9. Protection of embryo death by BWA in rHDL

A microinjection of CML (final 800 ng) into zebrafish embryos resulted in acute embryo death with up to 22±6% survivability at 24 hr-post injection (Figure 8A). In contrast, the PBS-alone injected embryo showed 73±3% survivability. In the presence of CML, the co-injection of rHDL-1 resulted in the highest survivability of the injected embryo, 63±3% ($p< 0.008$ vs. CML+PBS), whereas rHDL-0 showed 44±4% survivability ($p<0.032$ vs. CML+PBS). The co-injection of rHDL-0.5 resulted in 20% higher survivability than that of rHDL-0, approximately 53±5% survivability ($p<0.011$ vs. CML+PBS), suggesting that incorporation of BWA in rHDL enhanced the protective activity from acute embryo death in a dose-dependent manner. The rHDL-1 had remarkable protective activity against the CML-induced inflammatory death with the highest survivability.

Preprints (www.preprints.org) | NOT PEER-REVIEWED | Posted: 28 September 2023 doi:10.20944/preprints202309.2010.v1

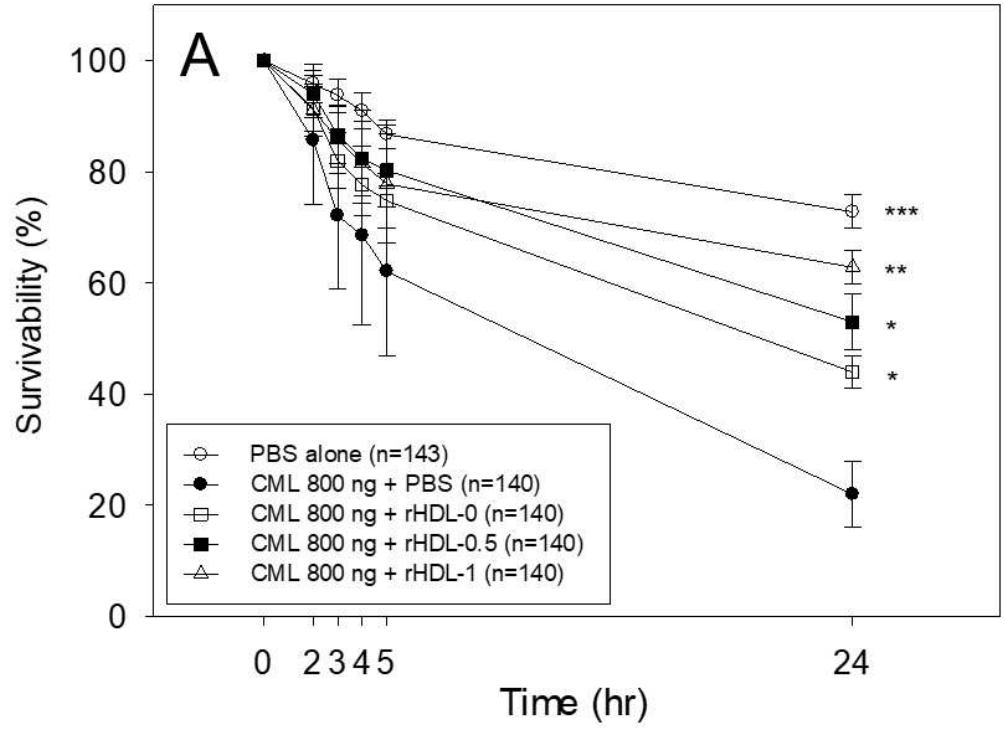

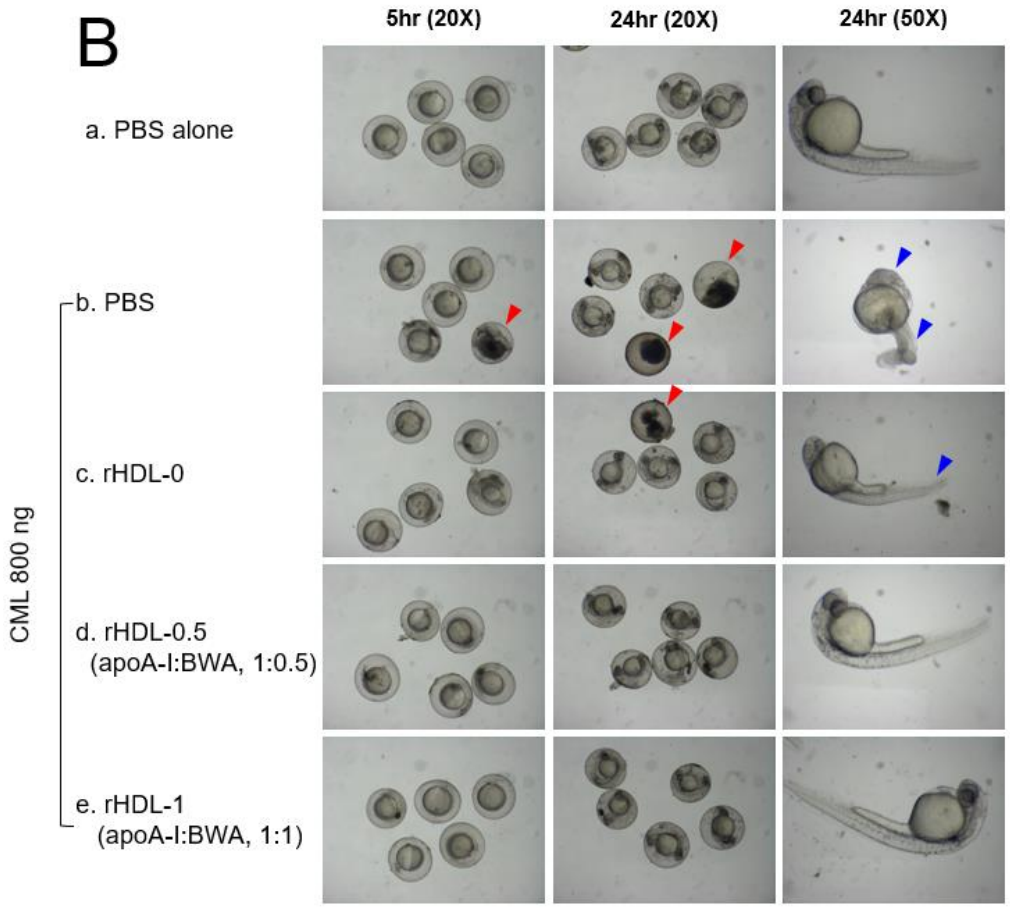

Preprints (www.preprints.org) | NOT PEER-REVIEWED | Posted: 28 September 2023 doi:10.20944/preprints202309.2010.v1

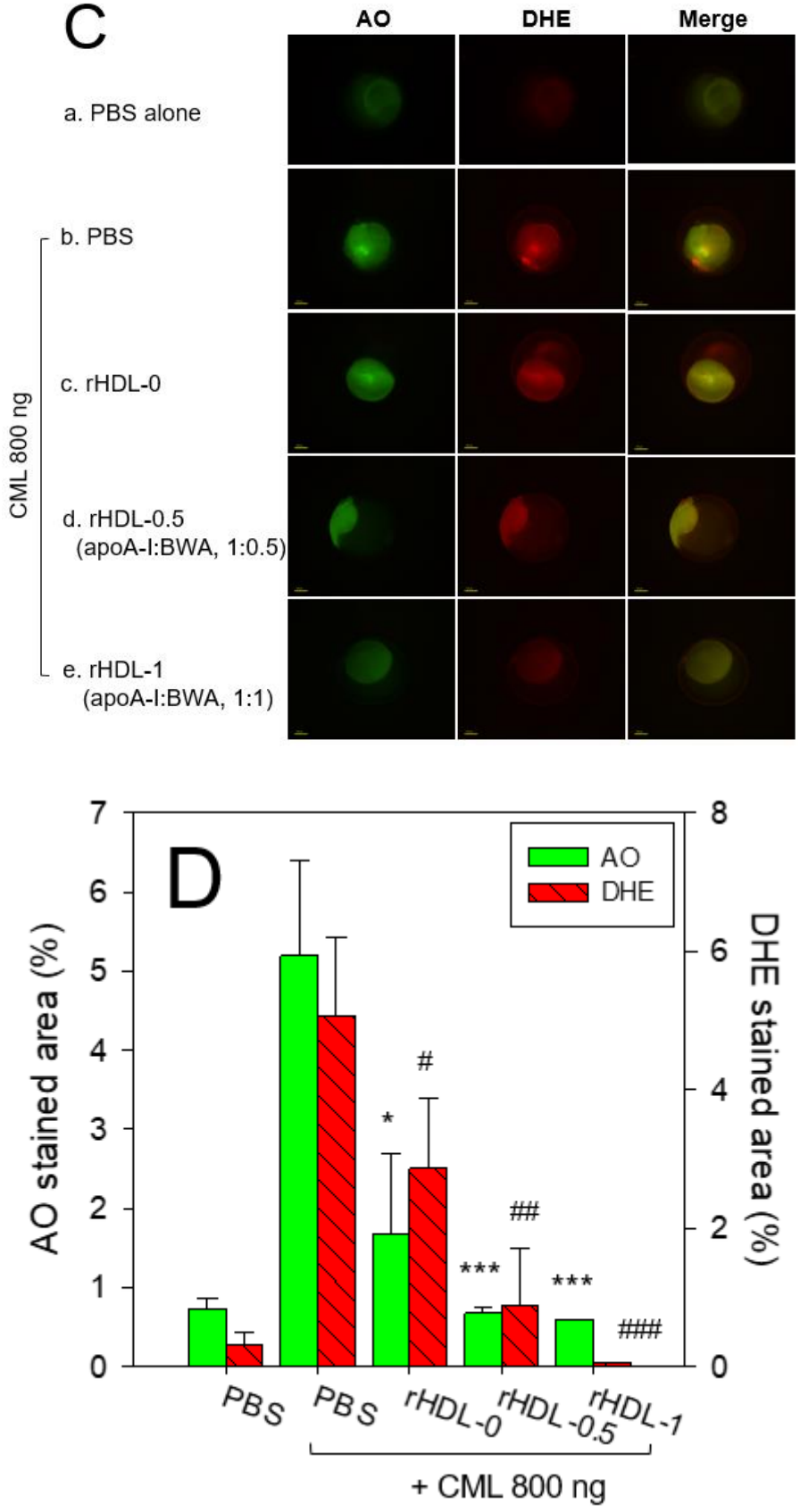

Figure 8. Comparison of survivability and embryo development among rHDLs containing BWA in the presence of carboxymethyllysine (CML, final 800 ng). A. Survivability of embryos during 24 hr post-injection of each rHDL and CML from three independent experiments. *, $p < 0.05$; **, $p < 0.01$; ***, $p < 0.05$ vs. CML alone. Statistical differences of multiple groups were compared using an independent

 doi:10.20944/preprints202309.2010.v1

t-test. B. Developmental morphology of the embryo at 5 hr and 24 hr post-injection. The red arrowheads indicate defects of development and death of embryos in the CML alone group (photo b) and CML + rHDL-0 (photo c). The blue arrowheads indicate the slowest developmental speed in eye pigmentation and tail elongation in the CML alone group (photo b) and CML + rHDL-0 group (photo c) at 24 h post-injection. C. Fluorescence image of acridine orange (AO, Ex = 505 nm, Em = 535 nm) stained and dihydroethidium (DHE, Ex=585 nm, Em=615 nm) stained embryo at 5 hr post-injection. The extent of apoptosis and ROS production was visualized by AO and DHE staining, respectively. D. Quantification of the fluorescence from AO-stained and DHE-stained embryo images using Image J software (http://rsb.info.nih.gov/ij/, accessed on 3 January 2023). The data are expressed as the mean±SD from five independent experiments. The statistical differences of multiple groups were compared using an independent *t*-test. a. PBS-alone injected; b. CML + PBS injected; c. CML + rHDL-0 injected; d. CML + rHDL-BWA (1:0.5) injected; e. CML + rHDL-BWA (1:1) injected. *, $p < 0.05$; ***, $p < 0.001$ vs. CML + PBS; #, $p < 0.05$; ##, $p < 0.01$; ###, $p < 0.001$ vs. CML + PBS.

The PBS-injected embryos (photo a) showed a normal developmental morphology and speed with eye pigmentation and tail elongation of more than 32 somites at 24 hr post-injection (Figure 8B). In comparison, the CML+PBS injected embryo (photo b) showed severe death and developmental defect (indicated by red arrowhead) with the weakest eye pigmentation and slowest tail elongation, less than 21 somites (indicated by blue arrowhead). On the other hand, a co-injection of rHDL-0 (photo c) improved the developmental morphology and speed with faster eye pigmentation and tail elongation (indicated by blue arrowhead), suggesting that rHDL alone could neutralize the CML toxicity in embryos to recover the developmental speed. Interestingly, a co-injection of rHDL-0.5 (photo d) and rHDL-1 (photo e) resulted in the most normal developmental speed and morphology, depending on the increase in the BWA molar ratio. The CML+rHDL-1 group showed the darkest eye pigmentation and tail elongation 24 hr-post injection.

AO staining showed that the CML-alone injected embryos had 8.7-fold higher green fluorescence (Figures 8C and 8D), suggesting that the CML injection caused acute apoptosis in embryos. In contrast, a co-injection of rHDL-1 decreased the apoptosis by up to 90.5% compared to the CML-alone group. The CML-alone-injected embryo also showed a 15.8-fold higher red fluorescence than the PBS-alone group from the DHE staining, indicating that apoptosis was accompanied by ROS production. A co-injection of rHDL-1 decreased the ROS levels by 98% compared to the CML-alone group. These results suggest that incorporating BWA into rHDL enhanced the antioxidant and anti-inflammatory activity to elevate embryo survivability in the presence of CML.

3.10. BWA in rHDL facilitated the healing of cutaneous wounds

Figure 9 presented the rHDL-aided cutaneous wound healing at different time points in the presence of CML. Wound healing appeared first at 4 hr post-treatment in the PBS, CML+rHDL-0, CML+rHDL-0.5, and CML+rHDL-1.0 treated groups. In contrast, no wound healing was observed in the CML-only treated group. The initial wound healing with 10.6% wound closer was observed in the PBS-treated group, followed by 8.9% wound closure in the CML+rHDL-0.5 treated group at 4 hr post-treatment. At 6 hr post-treatment, 5.7- and 4.2-fold higher wound healing was observed in the PBS and CML+rHDL-0.5 treated groups, respectively, compared to the CML-only treated group. The most noteworthy results were observed at 24 hours post-treatment, where 66% wound closure was observed in the PBS-treated group. Similarly, 57% wound closure was observed in the CML+rHDL-1-treated group, which was five-fold and 1.7-fold higher than that of the wound healing of the CML-only and CML+rHDL-0 treated groups, respectively. The utmost wound healing, with 86.4% wound closure, was observed in the CML+rHDL-1 group, which is higher than the PBS-alone group (~82.1% wound healing), followed by 78.4% wound closure in the CML+rHDL-0.5 treated group at 48 hr post-treatment. With the progression of time up to 48 hr post-treatment, a maximum wound healing was observed in the CML+rHDL-1 treated groups that are significantly two-fold ($p<0.001$) and 1.5-fold ($p<0.001$) higher than the wound closer observed in CML+ PBS and CML+rHDL-0 treated groups,

Preprints (www.preprints.org) | NOT PEER-REVIEWED | Posted: 28 September 2023 doi:10.20944/preprints202309.2010.v1

respectively. These results revealed the impact of BWA to ameliorate the rHDL wound healing activity against the CML-aggravated chronic wound.

The histology of the skin and muscle tissue of the wounded site was evaluated by H & E staining. The results revealed the development of the epidermis (neo-epithelization) in the PBS group (Figure 9). In contrast, a fragmented epidermis was observed in the CML and CML+rHDL-0 treated groups, indicating the role of CML in delaying wound closure. On the other hand, the CML co-treated with rHDL-0.5 and rHDL-1 groups showed remarkable epithelium development. Consequently, the wound closed. Furthermore, compact, muscular tissue, as indicated by the black arrow, appeared in the PBS group (Figure 9C), indicating the recovery of the wounded site. In contrast, a loosely packed muscular tissue documented the tissue injury in the CML-treated group. In contrast, the CML+ rHDL-0.5, and rHDL-1 treated groups showed much more organized and compact tissue, signifying the wound-healing role of rHDL-0.5 and rHDL-1.

DHE staining suggested ROS production at the wounded site. A massive ROS production was observed in the treated group, which was significantly 2.1-fold (p<0.05) higher than the ROS level in the PBS group (Figure 9). Similar to the treated group, the CML+rHDL-0 treated group did not affect the inhibition of ROS production. In contrast, the wounds treated with CML+rHDL-0.5 and rHDL-1 showed a significant decrease in ROS production compared to the CML-only treated group. The 1.5 fold (p<0.05) and 1.7 fold (p<0.05) lower ROS level in the rHDL-0.5 and rHDL-1 treated groups highlights the impact of rHDL-0.5 and rHDL-1 to diminish the ROS level, consequently progression of wound healing.

Consistent with DHE staining, AO staining also caused the highest apoptotic cell death in CML-treated wounded tissue, which was 2.3-fold (p<0.05) higher than that of the PBS-treated group (Figure 9C and 9D). The CML-induced apoptosis in the injured site was effectively countered by the rHDL-0.5 and rHDL-1, as evident by a significant 1.9-fold (p<0.05) and 3.0-fold (p<0.05) reduced the AO fluorescence intensity. These results collectively show that rHDL-0.5 and rHDL-1 efficiently inhibited the CML-induced ROS generation and subsequently inhibited apoptosis in the wounded site, leading to prompt wound recovery.

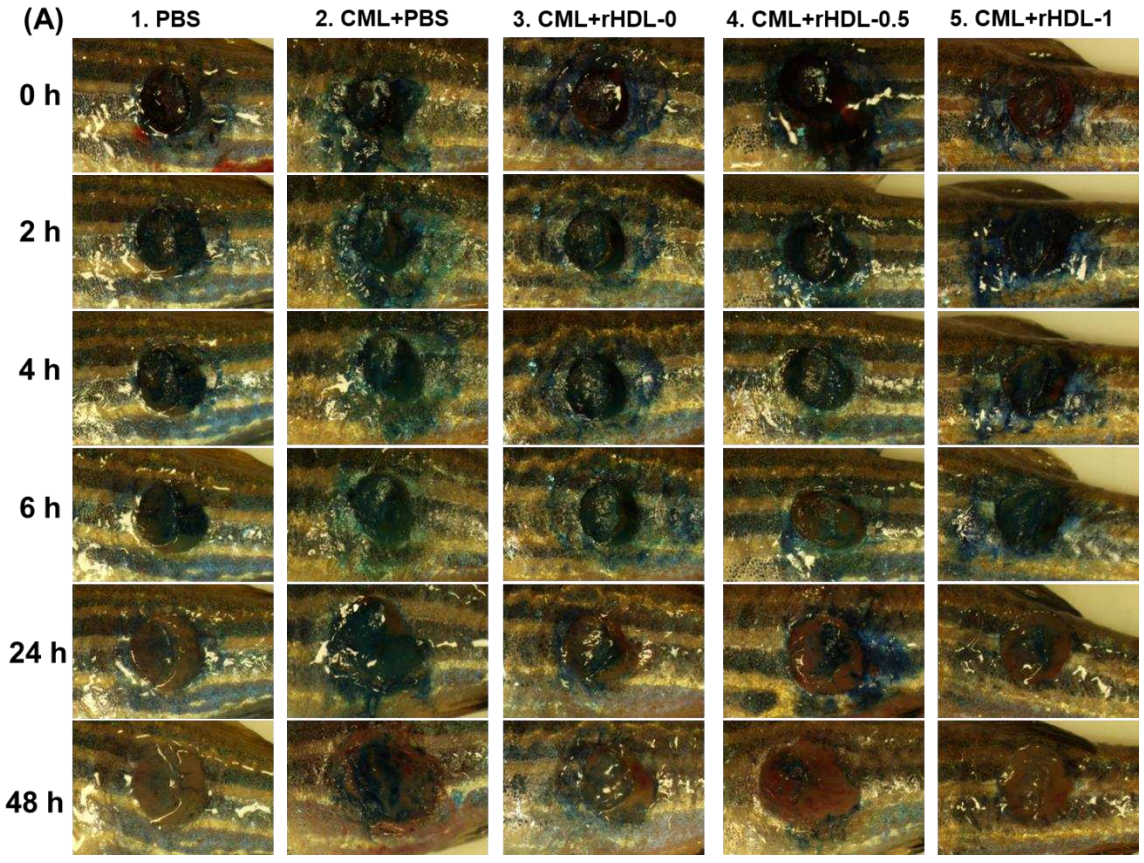

Preprints (www.preprints.org) | NOT PEER-REVIEWED | Posted: 28 September 2023 doi:10.20944/preprints202309.2010.v1

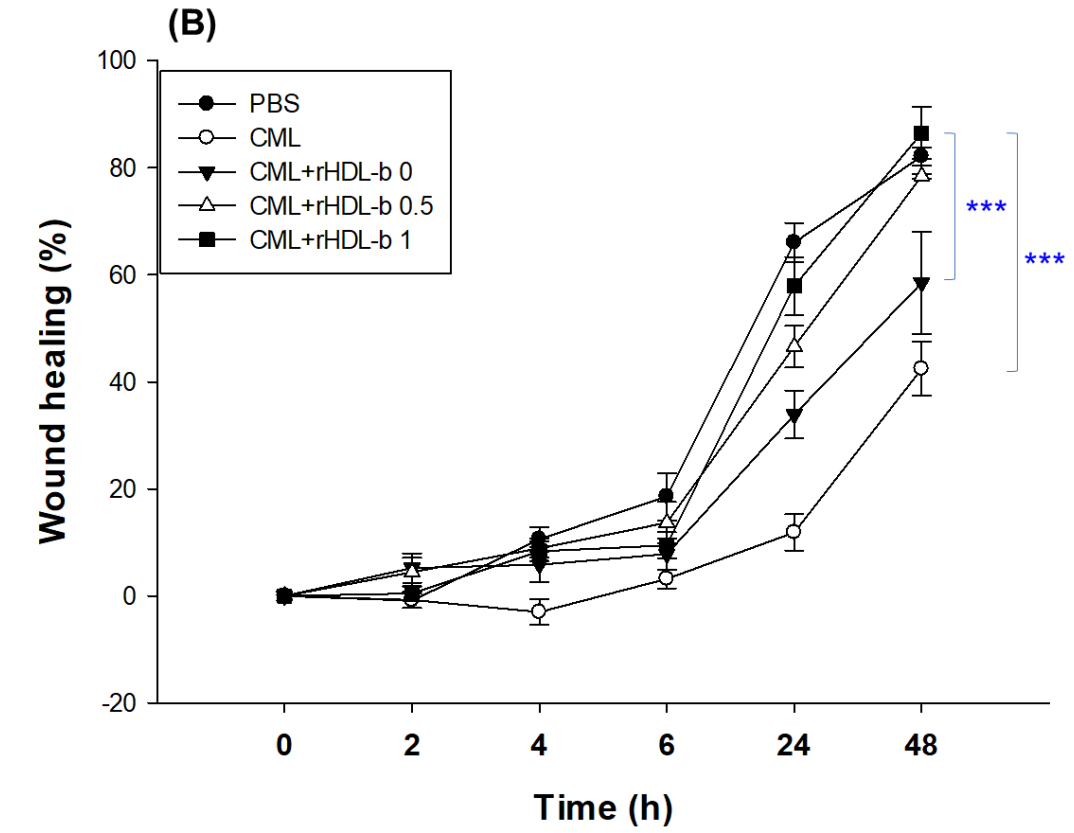

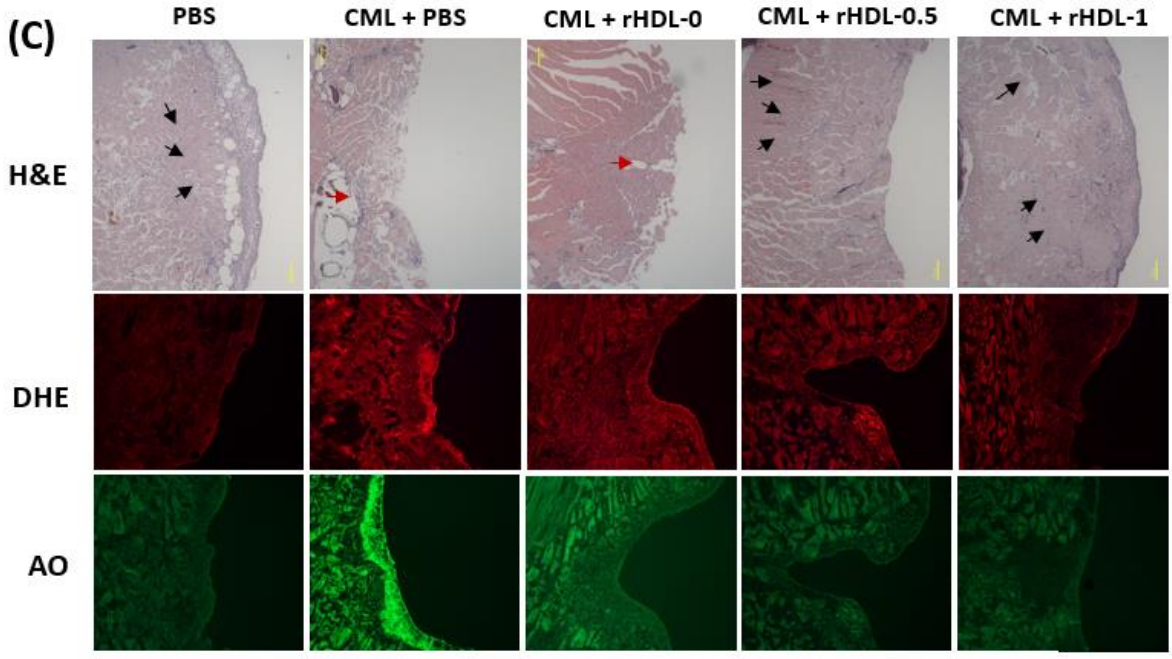

Preprints (www.preprints.org) | NOT PEER-REVIEWED | Posted: 28 September 2023 doi:10.20944/preprints202309.2010.v1

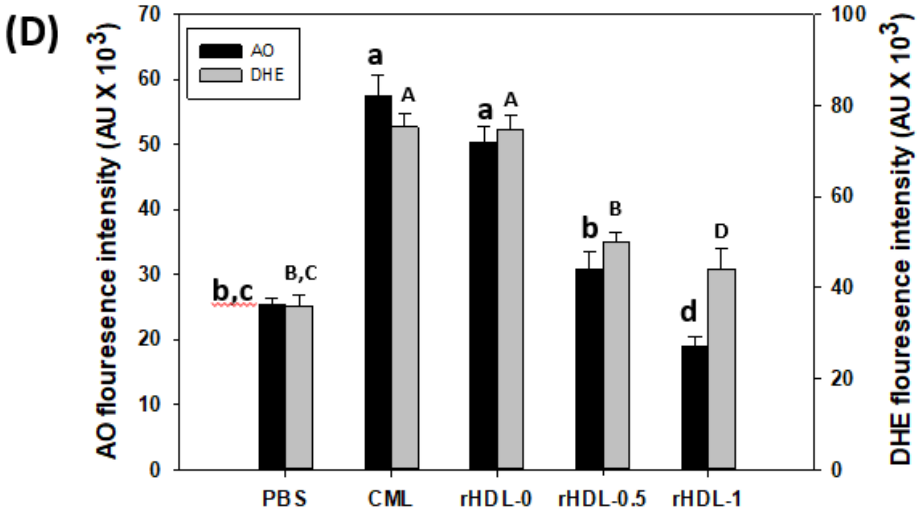

Figure 9. A comparative wound healing effect of rHDL composed of different proportions of beeswax alcohol (BWA) against carboxymethyllysine (CML) impaired cutaneous wound in zebrafish. **(A)** Pictorial view of the wounded area stained with methylene blue (0.1% (*w*/*v*) final). **(B)** A time-dependent wound healing up to 48 hours post-treatment. The wound healing was calculated by comparing the stained wound area measured at different time points against the wound stained area at 0 hr. P-value documented the pairwise statistical variance retrieved from the ANOVA using a Turkey test for Post Hoc analysis. **(C)** Hematoxylin and eosin (H& E) staining of the wounded tissue at 48 hours post-treatment**.** The black and red arrows indicate a compact and loosely packed muscular tissue, respectively. **(D)** Dihydroethidium (DHE) and acridine orange (AO) staining of the wounded tissue at 48 hr post-treatment. The fluorescent intensity in DHE and AO staining was measured using Image J software (version 1.53, http://rsb.info.nih.gov/ij/retrieved on 18 May 2023). The letters (a-d, A-D) above the bar charts indicate the significant statistical differences ($p<0.05$) among the groups.

4. Discussion

Oxidative damage in the lipid and proteins of the cell membrane surface can induce cellular necrosis and apoptosis through chemical and biophysical changes in the lipid bilayer components via necrotic cell signaling [35,36]. Lipid hydroperoxide-modified protein adducts, such as *N*®-(hexanoyl)lysine, were also found in oxLDL with a positive correlation with the extent of oxidation [37]. oxLDL could provoke acute cell death and foam cell formation by releasing pro-inflammatory cytokines to build up atherosclerotic plaque [38]. Therefore, inhibiting LDL oxidation is essential to prevent pro-inflammatory disease via suppressing ROS production, releasing adhesion molecules, the vicious cycle of inflammation, and apoptosis in the necrotic core while activating endothelial cells, smooth muscle cells, macrophages, and platelets [39]. On the other hand, the desirable antioxidant should protect HDL and apoA-I from oxidative modification, such as myeloperoxidase and lipoxygenase, and glycation stress, such as fructose and CML. Because HDL-associated paraoxonase activity is the principal power to exert inhibition of LDL oxidation, protection of HDL and apoA-I in the native state is essential for keeping the LDL healthy [40]. Dysfunctional HDL lost antioxidant and anti-inflammatory activity, such as paraoxonase activity, therefore, dysfunctional HDL cannot protect LDL from oxidative stress [41].

In general, lipid-soluble antioxidants protect cell membranes more efficiently from lipid peroxidation than water-soluble antioxidants, especially in oxidized lipids in the plasma membrane and inner membrane of mitochondria. Indeed, BWA in Tween 20 showed more potent inhibitory activity against LDL oxidation than that of vit C at lower concentrations (final 10–30 ◎M), as shown in Figure 1. Although vit C inhibited LDL oxidation by myeloperoxidase in vitro, the dosage was too high to use practical application, such as 50, 100, 150, and 200 mM [42]. In addition, vit C and E could not inhibit LDL oxidation by ferritin at lysosomal pH, which might help to explain why vit C and E

did not reduce CVD in large clinical trials [43]. Several phenolic compounds and flavonoids were developed as inhibitors of LDL oxidation [44]; new pharmaceutical agents are needed to maximize the antioxidant, anti-glycation, protection of HDL, and stabilization of apoA-I via an interaction of amphipathic helix domain. Hence, HDL functionality is more important in exerting the protective effects of HDL against cardiovascular risk than the HDL-C quantity [41]. Protection of apoA-I is critical to maintaining the antioxidant and anti-inflammatory activity of HDL because apoA-I (28 kDa) is the principal protein component in HDL particles [45]. Furthermore, apoA-I in a lipid-free state could exhibit antioxidant and anti-inflammatory activity, which can be impaired by nonenzymatic glycation [29,46].

This study was designed to compare the structural-functional correlations of reconstituted HDL with the increase in BWA content under the same apoA-I content and maximize the antioxidant capacity of BWA in an aqueous buffer. The apoA-I in rHDL was more stabilized as the molar ratio of apoA-I:BWA increased to approximately 1:1 (Figure 3). The rHDL particle morphology was changed to more distinct, and the size was larger (Figure 4). Regarding functionality, the anti-glycation ability of rHDL containing was enhanced with more protection of apoA-I and less glycation in HDL in the presence of fructose (Figure 5). The antioxidant ability of the rHDL was strengthened as the BWA molar ratio was increased to suppress cupric ion mediated LDL oxidation (Figure 6). The FRA and PON activities of human HDL were enhanced remarkably by the rHDL as the BWA content was increased (Figure 7). The rHDL containing BWA protected against embryo death from acute toxicity of CML by suppressing ROS production and apoptosis in a dose-dependent manner (Figure 8). BWA in rHDL facilitated cutaneous wound healing activity under CML toxicity in adult zebrafish (Figure 9).

To the best of the authors' knowledge, the current study is the first study to show that BWA could bind with apoA-I and cholesterol to construct rHDL, suggesting that the six even number long chain aliphatic alcohols (C24, C26, C28, C30, C32, and C34) made a putative affinity interaction with amphipathic helix domain of apoA-I. As the BWA concentration was increased, the particle size of rHDL increased up to 15% with a 1.5 nm redshift of intrinsic Trp, suggesting that the Trp in apoA-I was exposed more to the polar phase upon binding with BWA. Interestingly, this behavior of fluorophore movement differed from rHDL synthesis with policosanol (PCO) in a previous report [15]. A rHDL containing PCO (PCO-rHDL) showed a 1.9 nm blue shift of WMF, even though rHDL containing Cuban policosanol showed a 24% increase in particle diameter at 95:5:1:1 molar ratio for POPC:FC:apoA-I:PCO. The difference between BWA and PCO is two odd number aliphatic alcohols, C27 and C29 (1-hepacosanol and 1-nonacosanol, respectively), because policosanol is constituted with eight long chain aliphatic alcohols (C24, C26, C27, C28, C29, C30, C32, and C34). Although the incorporation of BWA and PCO caused an increase in the particle size of rHDL to a similar extent, but the movement of Trp in the amphipathic helix domain of apoA-I was different in the opposite direction. These results suggest that Trp108 of apoA-I showed different molecular motions and fluorophore environments between BWA-rHDL and PCO-rHDL by the putative interaction of C27 and C29. The intrinsic Trp108 was more exposed to the water phase BWA-rHDL, while PCO-rHDL showed more closed Trp108 toward the nonpolar phase of apoA-I. The BWA should have amphipathic properties between the water and lipid interfaces in the intercalated protein domain of the cell membrane to accomplish therapeutic activity for joint health benefits and gastroprotection.

On the other hand, the BWA-rHDL exerted stronger anti-glycation activity and antioxidant activity than rHDL alone, with an enhancement of the FRA and PON activities in HDL. Although many papers reported that BWA exhibited potent antioxidant and anti-inflammatory activity from animal and human serum after oral supplementation, no study has identified the beneficial in vitro activity because of the insolubility in water. These enhancements of in vitro antioxidant activity of HDL by BWA-rHDL are in good agreement with previous in vivo reports that showed a decrease in various oxidized lipids and enzymes involved in inflammation, such as COX-2, by apoA-I in colon cancer and ovarian cancer [47,48]. In the same context, the consumption of BWA (5–100 mg/kg) lowered carboxyl groups (a marker of protein oxidation) and the generation of hydroxyl (*OH) radical and myeloperoxidase (MPO) activity (a marker of inflammation), and increased the catalase

(CAT) activity in the gastric mucosa of rats with indomethacin ulcers [49]. Lipid peroxidation is critical to induce acute gastric mucosal injuries, pro-inflammatory cascades, and carcinogenesis [50,51].

Despite the many papers from animal and human studies showing that supplementation of BWA ameliorated gastric ulcers, esophagitis, and osteoarthritis [10,11,50], the in vitro antioxidant abilities of BWA and the mechanism of antioxidant activity after oral ingestion were not fully elucidated. Although BWA has adequate DPPH radical scavenging activity and ferric ion reduction ability in ethanol solvent assay systems [52], the current results showed that the incorporation of BWA in rHDL resulted in more enhancement of HDL-associated PON and FRA activity to inhibit LDL oxidation. The encapsulation of BWA in the rHDL is needed to maintain its antioxidant activity to suppress LDL oxidation because an organic solvent or non-ionic detergent, e.g., Tween 20, for BWA, might be toxic (Figure 1). The enforcement of HDL functionality by BWA encapsulation might be associated with the improvement of the barrier function by apoA-I stabilization (Figure 3 and 4), reduction of glycation stress (Figure 5) and oxidative stress (Figure 6 and 7), inhibition of embryonic cell apoptosis (Figure 7), and enhancement of wound healing (Figure 9). The enhancement of the HDL quality and functionality by BWA was associated with that of 17 days BWA supplementation (10% in diet, wt./wt.) in ameliorating the liver function and dyslipidemia to suppress interleukin-6 by increasing HDL functionality in the ethanol-induced hepatic injury zebrafish model [53].

5. Conclusion

The BWA can form discoidal rHDL via stabilization of apoA-I, which led to enhanced binding with apoA-I and a larger particle size. The BWA-rHDL exhibited enhanced anti-glycation, antioxidant, and anti-inflammatory abilities to protect HDL/apoA-I, which can suppress LDL oxidation and acute embryonic cell apoptosis.

Author Contributions: Conceptualization, K.-H.C.; methodology, H.-S.N., S-H. B., and A.B.; writing—original draft preparation, K.-H.C.; supervision, K.-H.C. All authors have read and agreed to the published version of the manuscript.

Funding: This research received no external funding.

Institutional Review Board Statement: The protocol for human blood donation was conducted according to the guidelines of the Declaration of Helsinki and was approved by the Korea National Institute for Bioethics Policy (KoNIBP, approval number P01-202109-31-009) supported by the Ministry of Health Care and Welfare (MOHW) of Korea.

Informed Consent Statement: Not applicable.

Data Availability Statement: The data used to support the findings of this study are available from the corresponding author upon reasonable request.

Conflicts of Interest: The authors declare no conflict of interest

References

1. Yeum, K. J., Russell, R. M., Krinsky, N. I., & Aldini, G. (2004). Biomarkers of antioxidant capacity in the hydrophilic and lipophilic compartments of human plasma. *Archives of biochemistry and biophysics*, *430*(1), 97–103. https://doi.org/10.1016/j.abb.2004.03.006
2. Pinchuk, I., Shoval, H., Dotan, Y., & Lichtenberg, D. (2012). Evaluation of antioxidants: scope, limitations and relevance of assays. *Chemistry and physics of lipids*, *165*(6), 638–647. https://doi.org/10.1016/j.chemphyslip.2012.05.003
3. Libardo MDJ, Wang TY, Pellois JP, Angeles-Boza AM. How Does Membrane Oxidation Affect Cell Delivery and Cell Killing? Trends Biotechnol. 2017 Aug;35(8):686-690. doi: 10.1016/j.tibtech.2017.03.015. Epub 2017 Apr 28. PMID: 28460718; PMCID: PMC5522782.
4. Dröge W. (2002). Free radicals in the physiological control of cell function. *Physiological reviews*, *82*(1), 47–95. https://doi.org/10.1152/physrev.00018.2001
5. Liguori I, Russo G, Curcio F, Bulli G, Aran L, Della-Morte D, Gargiulo G, Testa G, Cacciatore F, Bonaduce D, Abete P. Oxidative stress, aging, and diseases. Clin Interv Aging. 2018 Apr 26;13:757-772. doi: 10.2147/CIA.S158513. PMID: 29731617; PMCID: PMC5927356.

6. Leyane TS, Jere SW, Houreld NN. Oxidative Stress in Ageing and Chronic Degenerative Pathologies: Molecular Mechanisms Involved in Counteracting Oxidative Stress and Chronic Inflammation. Int J Mol Sci. 2022 Jun 30;23(13):7273. doi: 10.3390/ijms23137273. PMID: 35806275; PMCID: PMC9266760.
7. Lobo V, Patil A, Phatak A, Chandra N. Free radicals, antioxidants and functional foods: Impact on human health. Pharmacogn Rev. 2010 Jul;4(8):118-26. doi: 10.4103/0973-7847.70902. PMID: 22228951; PMCID: PMC3249911.
8. Ravelo, Y.; Molina, V.; Carbajal, D.; Fernández, L.; Fernández, J.C.; Arruzazabala, M.L.; Más, R. Evaluation of anti-inflammatory and antinociceptive effects of D-002 (beeswax alcohols). J. Nat. Med. 2011, 65, 330–335. [CrossRef] [PubMed]
9. Carbajal, D.; Molina, V.; Valdés, S.; Arruzazabala, M.d.L.; Más, R.; Magraner, J. Anti-inflammatory activity of D-002: An active product isolated from beeswax. Prostagland. Leukot. Essent. Fat. Acids 1998, 59, 235–238. [CrossRef] [PubMed]
10. Pérez, Y.; Oyárzabal, A.; Mas, R.; Molina, V.; Jiménez, S. Protective effect of D-002, a mixture of beeswax alcohols, against indomethacin-induced gastric ulcers and mechanism of action. J. Nat. Med. 2013, 67, 182–189. [CrossRef]
11. Puig, M.N.; Castaño, S.M.; Ferreiro, R.M.; Clara, M.V.; Hernansez, N.M. Effects of Oral Administration of D-002 (Beeswax Alcohols) on Histological and Functional Outcomes in a Rat Model of Antigen-Induced Arthritis: Preliminary Study. Int. J. Pharmacol. Phytochem. Ethnomed. 2016, 5, 60–68.
12. Molina V, Valdés S, Carbajal D, Arruzazabala L, Menéndez R, Mas R. Antioxidant effects of D-002 on gastric mucosa of rats with injury induced experimentally. *J Med Food.* 2001;4:79–84. [PubMed] [Google Scholar].
13. Pérez Y, Oyárzabal A, Mas R, Molina V, Jiménez S. Protective effect of D-002, a mixture of beeswax alcohols, against indomethacin-induced gastric ulcers and mechanism of action. *J Nat Med.* 2013;67:182–9.
14. Molina V, Mas R, Carbajal D. D-002 (beeswax alcohols): concurrent joint health benefits and gastroprotection. Indian J Pharm Sci. 2015 Mar-Apr;77(2):127-34. doi: 10.4103/0250-474x.156542. PMID: 26009643; PMCID: PMC4442459.
15. Cho, K. H., Baek, S. H., Nam, H. S., Kim, J. E., Kang, D. J., Na, H., & Zee, S. (2023). Cuban Sugar Cane Wax Alcohol Exhibited Enhanced Antioxidant, Anti-Glycation and Anti-Inflammatory Activity in Reconstituted High-Density Lipoprotein (rHDL) with Improved Structural and Functional Correlations: Comparison of Various Policosanols. *International journal of molecular sciences*, *24*(4), 3186. https://doi.org/10.3390/ijms24043186
16. Cho, K. H., Kim, J. E., Nam, H. S., Kang, D. J., & Na, H. J. (2022). Anti-Inflammatory Activity of CIGB-258 against Acute Toxicity of Carboxymethyllysine in Paralyzed Zebrafish via Enhancement of High-Density Lipoproteins Stability and Functionality. *International journal of molecular sciences*, *23*(17), 10130. https://doi.org/10.3390/ijms231710130
17. Sakata, N., Uesugi, N., Takebayashi, S., Nagai, R., Jono, T., Horiuchi, S., Takeya, M., Itabe, H., Takano, T., Myint, T., & Taniguchi, N. (2001). Glycoxidation and lipid peroxidation of low-density lipoprotein can synergistically enhance atherogenesis. *Cardiovascular research*, *49*(2), 466–475. https://doi.org/10.1016/s0008-6363(00)00262-5
18. Trede N.S., Zapata A., Zon L.I. Fishing for lymphoid genes. Trends Immunol. 2001;22:302–307. doi: 10.1016/S1471-4906(01)01939-1. - DOI - PubMed
19. Novoa B., Bowman T.V., Zon L., Figueras A. LPS response and tolerance in the zebrafish (Danio rerio) Fish Shellfish. Immunol. 2009;26:326e31. doi: 10.1016/j.fsi.2008.12.004.
20. Cho, K. H., Kim, J. E., Bahuguna, A., & Kang, D. J. (2023). Ozonated Sunflower Oil Exerted Potent Anti-Inflammatory Activities with Enhanced Wound Healing and Tissue Regeneration Abilities against Acute Toxicity of Carboxymethyllysine in Zebrafish with Improved Blood Lipid Profile. *Antioxidants (Basel, Switzerland)*, *12*(8), 1625. https://doi.org/10.3390/antiox12081625
21. Cho, K. H., Kim, J. H., Nam, H. S., & Kang, D. J. (2022). Efficacy Comparison Study of Human Epidermal Growth Factor (EGF) between Heberprot-P® and Easyef® in Adult Zebrafish and Embryo under Presence or Absence Combination of Diabetic Condition and Hyperlipidemia to Mimic Elderly Patients. *Geriatrics (Basel, Switzerland)*, *7*(2), 45. https://doi.org/10.3390/geriatrics7020045
22. Mas R. D-002: A product obtained from beeswax. Drugs Future 2001;26:731-44
23. Havel, R. J.; Eder, H. A.; Bragdon, J. H. The distribution and chemical composition of ultracentrifugally separated lipoproteins in human serum. *J. Clin. Invest.* **1955**, *34*, 1345-1353. [doi: 10.1172/JCI103182]
24. Brewer, H. B. Jr.; Ronan, R.; Meng, M.; Bishop, C. Isolation and characterization of apolipoproteins A-I, A-II, and A-IV. *Methods Enzymol.* **1986**, *128*, 223-246. [doi: 10.1016/0076-6879(86)28070-2]
25. Matz, C. E., & Jonas, A. (1982). Micellar complexes of human apolipoprotein A-I with phosphatidylcholines and cholesterol prepared from cholate-lipid dispersions. *The Journal of biological chemistry*, *257*(8), 4535–4540.
26. Markwell, M. A., Haas, S. M., Bieber, L. L., & Tolbert, N. E. (1978). A modification of the Lowry procedure to simplify protein determination in membrane and lipoprotein samples. *Analytical biochemistry*, *87*(1), 206–210. https://doi.org/10.1016/0003-2697(78)90586-9

27. Blois, M. S. Antioxidant determinations by the use of a stable free radical. *Nature* **1958**, *181*, 1199-1200. [doi: 10.1038/1811199a0]
28. Noble R. P. (1968). Electrophoretic separation of plasma lipoproteins in agarose gel. *Journal of lipid research*, *9*(6), 693–700.
29. McPherson, J. D.; Shilton, B. H.; Walton, D. J. Role of fructose in glycation and cross-linking of proteins. *Biochemistry* **1988**, *27*, 1901-1907. [doi: 10.1021/bi00406a016]
30. Nusslein-Volhard, C.; Dahm, R. Zebrafish: A Practical Approach, 1st ed.; Oxford University Press: Oxford, UK, 2002.
31. National Research Council of the National Academy of Sciences. Guide for the Care and Use of Laboratory Animals; National Academy Press: Washington, DC, USA, 2010.
32. Cho, K. H., Nam, H. S., Kim, J. E., Na, H. J., Del Carmen Dominguez-Horta, M., & Martinez-Donato, G. (2023). CIGB-258 Exerts Potent Anti-Inflammatory Activity against Carboxymethyllysine-Induced Acute Inflammation in Hyperlipidemic Zebrafish via the Protection of Apolipoprotein A-I. *International journal of molecular sciences*, *24*(8), 7044. https://doi.org/10.3390/ijms24087044
33. Owusu-Ansah, E.; Yavari, A.; Mandal, S.; Banerjee, U. Distinct mitochondrial retrograde signals control the G1-S cell cycle checkpoint. *Nat. Genet.* **2008**, *40*, 356–361. https://doi.org/10.1038/ng.2007.50.
34. Hayashi, M., Sofuni, T., & Ishidate, M., Jr (1983). An application of Acridine Orange fluorescent staining to the micronucleus test. *Mutation research*, *120*(4), 241–247. https://doi.org/10.1016/0165-7992(83)90096-9
35. Hanus J, Zhang H, Wang Z, Liu Q, Zhou Q, Wang S. Induction of necrotic cell death by oxidative stress in retinal pigment epithelial cells. Cell Death Dis. 2013 Dec 12;4(12):e965. doi: 10.1038/cddis.2013.478. PMID: 24336085; PMCID: PMC3877549.
36. Libardo, M. D. J., Wang, T. Y., Pellois, J. P., & Angeles-Boza, A. M. (2017). How Does Membrane Oxidation Affect Cell Delivery and Cell Killing?. *Trends in biotechnology*, *35*(8), 686–690. https://doi.org/10.1016/j.tibtech.2017.03.015
37. Kato, Y., Mori, Y., Makino, Y., Morimitsu, Y., Hiroi, S., Ishikawa, T., & Osawa, T. (1999). Formation of Nepsilon-(hexanonyl)lysine in protein exposed to lipid hydroperoxide. A plausible marker for lipid hydroperoxide-derived protein modification. *The Journal of biological chemistry*, *274*(29), 20406–20414. https://doi.org/10.1074/jbc.274.29.20406
38. Pirillo A, Norata GD, Catapano AL. LOX-1, OxLDL, and atherosclerosis. Mediators Inflamm. 2013;2013:152786. doi: 10.1155/2013/152786.
39. Duan, H., Song, P., Li, R., Su, H., & He, L. (2023). Attenuating lipid metabolism in atherosclerosis: The potential role of Anti-oxidative effects on low-density lipoprotein of herbal medicines. *Frontiers in pharmacology*, *14*, 1161657. https://doi.org/10.3389/fphar.2023.1161657
40. Kosmas CE, Martinez I, Sourlas A, Bouza KV, Campos FN, Torres V, Montan PD, Guzman E. High-density lipoprotein (HDL) functionality and its relevance to atherosclerotic cardiovascular disease. Drugs Context. 2018 Mar 28;7:212525. doi: 10.7573/dic.212525. PMID: 29623098; PMCID: PMC5877920.
41. Cho K. H. (2022). The Current Status of Research on High-Density Lipoproteins (HDL): A Paradigm Shift from HDL Quantity to HDL Quality and HDL Functionality. *International journal of molecular sciences*, *23*(7), 3967. https://doi.org/10.3390/ijms23073967
42. Samsam Shariat SZ, Mostafavi SA, Khakpour F. Antioxidant effects of vitamins C and e on the low-density lipoprotein oxidation mediated by myeloperoxidase. Iran Biomed J. 2013;17(1):22-8. doi: 10.6091/ibj.1092.2012. PMID: 23279831; PMCID: PMC3600973.
43. Ojo, O. O., & Leake, D. S. (2021). Vitamins E and C do not effectively inhibit low density lipoprotein oxidation by ferritin at lysosomal pH. *Free radical research*, *55*(5), 525–534. https://doi.org/10.1080/10715762.2021.1964494
44. Amarowicz, R., & Pegg, R. B. (2017). The Potential Protective Effects of Phenolic Compounds against Low-density Lipoprotein Oxidation. *Current pharmaceutical design*, *23*(19), 2754–2766. https://doi.org/10.2174/1381612823666170329142936
45. Barter, P. J., Nicholls, S., Rye, K. A., Anantharamaiah, G. M., Navab, M., & Fogelman, A. M. (2004). Antiinflammatory properties of HDL. *Circulation research*, *95*(8), 764–772. https://doi.org/10.1161/01.RES.0000146094.59640.13
46. Nobécourt, E., Tabet, F., Lambert, G., Puranik, R., Bao, S., Yan, L., Davies, M. J., Brown, B. E., Jenkins, A. J., Dusting, G. J., Bonnet, D. J., Curtiss, L. K., Barter, P. J., & Rye, K. A. (2010). Nonenzymatic glycation impairs the antiinflammatory properties of apolipoprotein A-I. *Arteriosclerosis, thrombosis, and vascular biology*, *30*(4), 766–772. https://doi.org/10.1161/ATVBAHA.109.201715
47. Aguirre-Portoles, C.; Feliu, J.; Reglero, G.; Ramirez de Molina, A. ABCA1 overexpression worsens colorectal cancer prognosis by facilitating tumour growth and caveolin-1-dependent invasiveness, and these effects can be ameliorated using the BET inhibitor apabetalone. Mol. Oncol. **2018**, 12, 1735–1752. [CrossRef]
48. Gao, F.; Chattopadhyay, A.; Navab, M.; Grijalva, V.; Su, F.; Fogelman, A.M.; Reddy, S.T.; Farias-Eisner, R. Apolipoprotein A-I mimetic peptides inhibit expression and activity of hypoxia-inducible factor-1alpha in

human ovarian cancer cell lines and a mouse ovarian cancer model. J. Pharmacol. Exp. Ther. **2012**, 342, 255–262. [CrossRef] [PubMed]

49. 49..Pérez Y, Oyárzabal A, Mas R, Molina V, Jiménez S. Protective effect of D-002, a mixture of beeswax alcohols, against indomethacin-induced gastric ulcers and mechanism of action. *J Nat Med*. 2013;67:182–9. [PubMed] [Google Scholar]
50. Naito, Y., Takagi, T., Handa, O., & Yoshikawa, T. (2014). Lipid hydroperoxide-derived modification of proteins in gastrointestinal tract. *Sub-cellular biochemistry*, *77*, 137–148. https://doi.org/10.1007/978-94-007-7920-4_12
51. Naito, Y., Yoshikawa, T., Yoshida, N., & Kondo, M. (1998). Role of oxygen radical and lipid peroxidation in indomethacin-induced gastric mucosal injury. *Digestive diseases and sciences*, *43*(9 Suppl), 30S–34S.
52. Puente R, Illnait J, Mas R, Carbajal D, Mendoza S, Fernández JC, Mesa M, Gámez R, Reyes P. Evaluation of the effect of D-002, a mixture of beeswax alcohols, on osteoarthritis symptoms. Korean J Intern Med. 2014 Mar;29(2):191-202. doi: 10.3904/kjim.2014.29.2.191. Epub 2014 Feb 27. PMID: 24648802; PMCID: PMC3956989.
53. Han, Y., Zee, S., & Cho, K. H. (2023). Beeswax Alcohol and Fermented Black Rice Bran Synergistically Ameliorated Hepatic Injury and Dyslipidemia to Exert Antioxidant and Anti-Inflammatory Activity in Ethanol-Supplemented Zebrafish. *Biomolecules*, *13*(1), 136. https://doi.org/10.3390/biom13010136